Chem Soc Rev

REVIEW ARTICLE

View Article Online
View Journal | View Issue

Cite this: *Chem. Soc. Rev.*, 2023, **52**, 2688

Functional chromopeptide nanoarchitectonics: molecular design, self-assembly and biological applications

Rui Chang,†[a] Luyang Zhao,†[a] Ruirui Xing,*[ab] Junbai Li *[c] and Xuehai Yan *[abd]

Chromoproteins are a class of delicate natural compounds that elegantly complex photosensitive species with proteins and play a central role in important life processes, such as photosynthesis. Inspired by chromoproteins, researchers integrate simple peptides and photosensitive molecular motifs to generate chromopeptides. Compared with chromoproteins, chromopeptides exhibit a relatively simple molecular structure, flexible and adjustable photophysical properties, and a capability of programmable self-assembly. Chromopeptide self-assembly has attracted great attention as the resultant high-level architectures exhibit an ingenious combination of photofunctions and biofunctions. This review systematically summarizes recent advances in chromopeptide nanoarchitectonics with particular focus on the design strategy, assembly mechanism, and structure–function relationship. Among them, the effect of peptide sequences and the variation in photophysical performance are critically emphasized. On this basis, various applications, including biomedicine and artificial photosynthesis, are discussed together with the future prospects of chromopeptide nanoarchitectonics. This review will provide insights into chromopeptide nanoarchitectonics and corresponding materials with precise designs, flexible nanostructures and versatile functions. In addition, knowledge involving chromopeptide nanoarchitectonics may aid in the development of many other kinds of supramolecular biological materials and bioengineering techniques.

Received 25th December 2022

DOI: 10.1039/d2cs00675h

rsc.li/chem-soc-rev

[a] *State Key Laboratory of Biochemical Engineering, Institute of Process Engineering, Chinese Academy of Sciences, Beijing 100190, P. R. China. E-mail: rrxing@ipe.ac.cn, yanxh@ipe.ac.cn*
[b] *School of Chemical Engineering, University of Chinese Academy of Sciences, Beijing 100049, P. R. China*
[c] *Beijing National Laboratory for Molecular Sciences, CAS Key Lab of Colloid, Interface and Chemical Thermodynamics Institute of Chemistry, Chinese Academy of Sciences Beijing, 100190, P. R. China. E-mail: jbli@ipe.ac.cn*
[d] *Center for Mesoscience, Institute of Process Engineering, Chinese Academy of Sciences, Beijing 100190, P. R. China*
† These authors contributed equally to this work.

Rui Chang

Rui Chang received her PhD degree from the Institute of Process Engineering (IPE), University of Chinese Academy of Sciences (UCAS), in 2022; then she started post-doctoral research at the Institute of Process Engineering (IPE), Chinese Academy of Sciences (CAS), under the supervision of Prof. Yan in the same year. Her research interests are mainly focused on peptide-based nanodrugs and their application in the area of antitumor theranostics, especially phototherapy and immunotherapy.

Luyang Zhao

Luyang Zhao received his PhD degree in chemistry in 2016 from the University of Science and Technology Beijing. He then joined Prof. Xuehai Yan's group as a postdoc at the State Key Laboratory of Biochemical Engineering, IPE, CAS, and became an associated professor in 2019. His research interests are focused on the design of peptide-based bioactive molecules and self-assembling photosensitive materials.

1 Introduction

Natural compounds and their organization provide inspiration for new and fascinating opportunities to develop innovative biomaterials.[1–3] Chromoproteins are a class of functional proteins bearing a chromophoric group, which are used as building blocks for achieving diversified nanoarchitectonics and creating high functional systems similar to biological systems.[4–6] Typical examples of natural chromoproteins include the fluorescent protein family, haemoglobin, flavoproteins, ferritin, and chloroplastin.[7–9] These proteins are characterized by electronic absorption in the visible or near-infrared (NIR) spectral range and may serve as enzymes, photoreceptors, photocatalysts or electron transferring elements. Chromopeptides, which are derived from chromoproteins, integrate the programmable flexibility of peptide motifs and optical functions of chromophores, showing an ingenious combination of peptide and chromophore properties.

Chromopeptides are structurally simplified analogues of chromoproteins, which perform synergistic functions similar to those of natural chromoproteins. For example, actinomycin D, also named dactinomycin, is a natural chromopeptide composed of a heterocyclic chromophore and two cyclic pentapeptide lactone rings.[10] The compound functions as a transcription inhibitor and prevents RNA polymerase elongation. Chromopeptide, as its name implies, is composed of a peptide motif and a chromophore, in which the peptide motif is covalently or noncovalently coupled with a chromophore, such as porphyrins, cyanines and anthocyanins. Compared to chromoproteins, chromopeptides have relatively simple chemical structures, flexible and adjustable photophysical properties, and capabilities of programmable self-organization.

Since as early as the 1990s, very extensive attention has been directed to chromopeptides with biomimetic and phototherapeutic functions. For example, a series of synthetic analogues of heme proteins, called heme–peptide complexes, have been synthesized to elucidate the inherent structure–function relationship of natural heme proteins and their catalytic functions.[11–13] As a simplified model, the heme–peptide complex provides a fundamental explanation of the molecular mechanisms of heme protein reactions and mimics the O_2 binding, activation and hydrocarbon hydroxylation chemistry processes with haemoglobin, peroxidase, and cytochrome P450. During the following years, a vast number of research studies focused on the design and synthesis of covalently linked photosensitizer–peptide conjugates to achieve precise and effective phototherapy against tumours.[14–18] The porphyrin and chlorin parent compounds constitute the base of many potent photosensitizers for clinical photodynamic therapy (PDT). However, many of these compounds exhibit drawbacks, such as cytotoxicity, limited permeability and low targeting ability.[19–22] Peptides are most commonly used for enhancing photosensitizer targeting specificity and decreasing nonspecific phototoxicity because their synthesis process is straightforward and they are easily conjugated to photosensitizers.[23,24] These chromopeptides, also called third-generation photosensitizers, have shown increased PDT efficacy compared with that of unconjugated photosensitizers.

Chromopeptide self-assembly based on the principles of nanoarchitectonics is an important strategy for designing a wide spectrum of functional biomimetic materials and devices for nanomedicine and nanobiotechnology.[23,25,26] For example, in organisms, a growing number of bacterially secreted proteins self-assemble and form fibrillar amyloid-like nanostructures to

Ruirui Xing

Ruirui Xing is currently an associate professor at the Institute of Process Engineering (IPE), CAS. Her research interests are focused on the design and self-assembly of functional peptides, supramolecular effects, nanomaterials and nanodrugs, and applications in the field of biomedicine.

Junbai Li

Junbai Li is a professor at the Institute of Chemistry in the Chinese Academy of Sciences. His research interests include molecular biomimetics based on molecular assembly, reconstitution of motor proteins, self-assembly of dipeptides, biointerfaces, bioinspired materials, and nanostructure design.

Xuehai Yan

Xuehai Yan is a full professor at the Institute of Process Engineering, Chinese Academy of Sciences (CAS). Currently, he is the deputy director of the State Key Laboratory of Biochemical Engineering and the Center of Mesoscience, IPE, CAS. His research interests are focused on peptide self-assembly and engineering, supramolecular colloids and crystals, phase evolution and dynamic transition, as well as cancer phototherapy and immunotherapy.

fight infections. In chlorosomes, biopigments self-assemble into large supramolecular structures to capture light and transfer energy. Inspired by the self-assembly behaviour in biological systems, efforts have been devoted to exploring the self-assembly process of well-designed small biological molecules. The self-assembly process of amino acid-encoded peptides (such as ion-complementary peptides,[27] amphiphilic peptides,[28,29] aromatic peptides,[30] and cyclic peptides[31]) has led to the formation of various well-ordered nanostructures that accurately mimic the function of natural proteins. However, the peptide building blocks reported previously seldom involved in the introduction of biologically derived chromophores and the fabrication of corresponding nanomaterials.[28,30,32,33] As a new family of peptide building blocks, chromopeptide self-assembly provides an ingenious combination of peptide and chromophore properties as well as synergistic functions that are inaccessible to individual molecular units.[34,35] In recent years, we have witnessed increasing work on the self-assembly of chromopeptides and their unique functions and potential applications, ranging from light harvesting and biomimetic catalysis to cancer diagnosis and treatment. However, despite numerous highly innovative and original studies, advances in chromopeptide self-assembly have not been summarized.

In this review, we present the self-assembly of chromopeptides, with a focus on the molecular design, assembly process control, structure regulation, function integration and biological applications of chromopeptide-based assembly materials (Fig. 1). The first section introduces the molecular strategies of designing chromopeptides, including the following typical combination types between the chromophores and peptide motifs: noncovalent combination and covalent conjugation. The second section describes principles and examples on how to regulate the self-assembly process, the resulting supramolecular structures and their functions. The following section covers the potential applications of chromopeptide assemblies, such as imaging, phototherapy, biomimetic photocatalysis and photosynthesis. With an overview of chromopeptide nanoarchitectonics, we can systematically understand this kind of new emerging peptide building blocks. More importantly, this review presents a versatile tool to develop functional biomimetic materials for a variety of applications.

2 Molecular design principles for chromopeptides

Chromoproteins are composed of chromophores and protein segments, mostly conjugated in a noncovalent manner.[36] Chromoprotein complexes based on self-assembly or aggregation of chromoproteins are naturally occurring complexes with unique features. One typical example is the purple bacterial antenna complex system, in which 9 α/β-apoprotein pairs are assembled on a cylinder with a hollow radius of 14 Å and an outer wall radius of 34 Å. Inside each α/β-apoprotein pair are bound three NIR bacteriochlorophylls (BChl) with histidines from α-(His 31) and β-(His 30). The BChls in the complex system form an overlapped ring-like supramolecular structure, which facilitates efficient light harvesting and electron transfer.[37] In many cases, the chromophores inside the chromoprotein supramolecular structure are either single molecular units or arranged in a definite but loosely-packed pattern, which depends on the functions of the chromoprotein.[4,38]

Comparably, chromopeptides are much more flexible in molecular composition and can be obtained *via* both covalent and noncovalent bonds.[7,39] Besides, the chromophore motifs in the chromopeptide may have stronger interaction and closer attachment with each other than those in chromoprotein. By designing chromopeptide molecules and assembling well-defined supramolecular structures, multiple unique physical properties and novel functionalities can be achieved. This section summarizes the molecular design principles together with the self-assembled structures of chromopeptides.

2.1 Noncovalent assembly of chromophores and peptides as building blocks

Similar to chromoprotein, as a biomimetic case, the chromophore and peptide building blocks are noncovalently coassembled. The noncovalent combination provides maximal

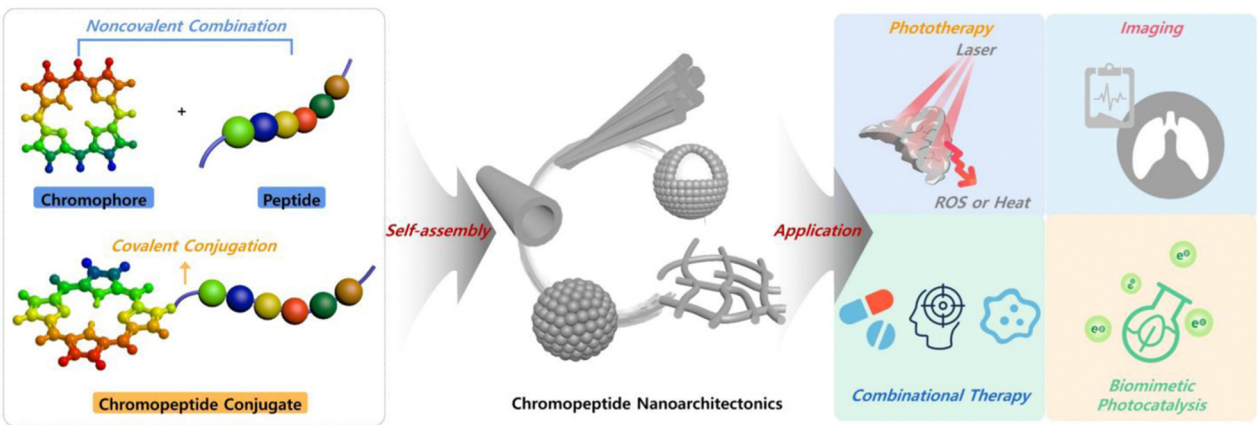

Fig. 1 Schematic representation of the chromopeptide molecular structure, self-assembly and representative biological applications.

freedom for each motif during assembly,[40,41] and the resulting supramolecular assemblies may exhibit diverse nanostructures, morphologies and properties, which are not only dependent on the intrinsic properties of each component, but can also be regulated by the sequence of the peptide motif, the noncovalent binding site, the molar ratio between building blocks, and many other environmental conditions as well as external species.

The coassembly of chromophores and polypeptides with charged repeating residues has been demonstrated to be efficient in inducing J-aggregate formation. One example is the coassembly of poly(L-Lys) and sulfonated porphyrin(tetrakis(4-sulfonatophenyl) porphine (TPPS)), yielding rod-like assemblies.[42,43] In addition, the coassembly of chromophores and peptide dendrimers with well-defined and controllable end groups has been shown to produce higher ordered structures. For example, a natural zinc(ii) porphyrin derivative Zn–mesoporphyrin IX coordinates with the well-designed peptide dendrimer to generate assemblies of porphyrin–dendrimers and realizes enhanced electron transfer, which is mainly because the porphyrins stack more densely in the peptide dendrimers and the light energy delocalizes better.[44,45]

Importantly, the coassembly between peptides and chromophores may be controlled precisely and flexibly. Fry *et al.* reported that self-assembly of an amphliphilic octapeptide with an *N*-palmitoyl group, namely, c16-AHL$_3$K$_3$, in neutral aqueous media afforded micelles with an average diameter of 6 nm. Whereas by introducing a natural heme derived chromophore, (PpIX)Zn, which was chosen to mimic natural light-harvesting species, micelles still formed and their size grew from 6 nm to 30 nm along with the molar ratio between chromophores and peptides increasing from 1 : 60 to 1 : 6.[46] The change in micellar size is considered to be occurring due to the competing interactions. In the absence of (PpIX)Zn, the micelles form due to the presence of a hydrophobic palmitoyl core and electrostatic repulsion between the neighboring positively charged lysine. Upon incorporating (PPIX)Zn, additional forces are introduced: (1) electrostatic attraction between lysine and the negatively charged carboxyl moieties on the macrocycle and (2) Zn–histidine coordination. Probably, the former dominantly contributes to the micelle size enlargement. Meanwhile, the coassembly morphologies were influenced by the solution pH and the peptide sequence.[47] Taking the pH value as an example, the micelle at pH = 7 spontaneously converted to fibres with the pH increasing to 11. Herein, the high pH close to the pK_a of lysine reduces electrostatic repulsion, shortening the distances between individual peptide molecules to a van der Waals range. Synergistically, leucines assist in the formation of long-aspect ratio nanofibers by serving as a β-sheet structural motif. These coassembly conditions have great impacts on the spin states of (PpIX)Zn. As a consequence, the photophysical properties together with its resulting catalytic activities can be finely tuned by coassembling with peptides.

Remarkably, the coassemly morphology is varied if the chromophore is in a relatively high concentration. Yan *et al.* represented a hierarchical assembly scenario of dipeptides and TPPS with a defined molar ratio.[48] In an acidic solution, the dipeptide, diphenylalanine (FF), is a singly charged cation ($[FF]^+$), and TPPS is dianionic ($[H4TPPS]^{2-}$). Coassembly of TPPS and FF led to the formation of a porous microsphere with a molar ratio of 2.3 : 1, consistent with the charge-neutralized 2 : 1 dipeptide–porphyrin ionic complex. The formation of microspheres occurred in two sequential steps as follows: driven by the π–π interactions between intermolecular TPPS molecules, TPPS first assembled to form an ordered J-aggregation structure; and then, driven by the electrostatic interaction between $[FF]^+$ and $[H4TPPS]^{2-}$, a spherical structure with porosity, multiple chambers and a high degree of hydration was eventually formed (Fig. 2A–C). Interestingly, the microassembly morphology drastically varies depending on the peptide properties. Substituting amphiphilic FF with hydrophilic dilysine (KK) afforded a hierarchically organized fibre bundle.[49] The coassembly of hydrophilic KK and porphyrin also preferentially formed nanorod-shaped J-aggregates *via* strong π–π interactions of TPPS at the beginning and then spontaneously grouped into fibre bundles with anisotropic birefringence and photoluminescence; this occurred due to the synergistic effects between long-range electrostatic repulsion and short-range van der Waals attraction (Fig. 2A, D and E). The coassembled nanoplatforms exhibited remarkable differences in their nanostructure morphologies, which was attributed to the difference in the hydrophilic and hydrophobic properties of the peptides. FF molecules show strong hydrophobicity and tend to insert into the interior of the porphyrin J-aggregate structure, while hydrophilic KK molecules tend to be fixed on the surface of porphyrin J-aggregates, thus enhancing the directivity of porphyrin nanorods and promoting the directional growth of nanorods into the fibre bundle structure (Fig. 2A). These results also indicated that organic chromophores like porphyrin at a high concentration usually form strong π–π interactions, and thus prefer aggregation to oligomers before coassembly with peptides. Compared with the porphyrin alone, the chromopeptide system exhibits much enhanced resistance to photodegradation and potential applications such as light-harvesting antennae and sustainable photocatalytic activity.

2.2 Self-assembly of molecular chromopeptide conjugates

Since chemical modification of peptides is facile, the chromophore and peptide segments could also be covalently conjugated and integrated into a new molecular building block. Herein, the chromophore is selected or designed by considering its unique functions like fluorescence, photodynamic activity, photothermal conversion, photocatalysis, and so forth. The peptide is adopted based on both its biological activity and its properties on tuning assembly. Depending on their photophysical properties and biological activities, the compounds can be directly conjugated or spaced with a linking group. Different covalent conjugation strategies lead to various assembled nanostructures, as classified in the following subsections.

2.2.1 Direct conjugation of the chromophore and peptide segments. In this manner, the chromophore and peptide segments are conjugated *via* covalent bonds, and the conjugation may be at the N-, C-, or residue terminal of the peptide. Chromophores and their derivatives, such as porphyrin-based chromophores, biliverdin or indocyanine, usually contain

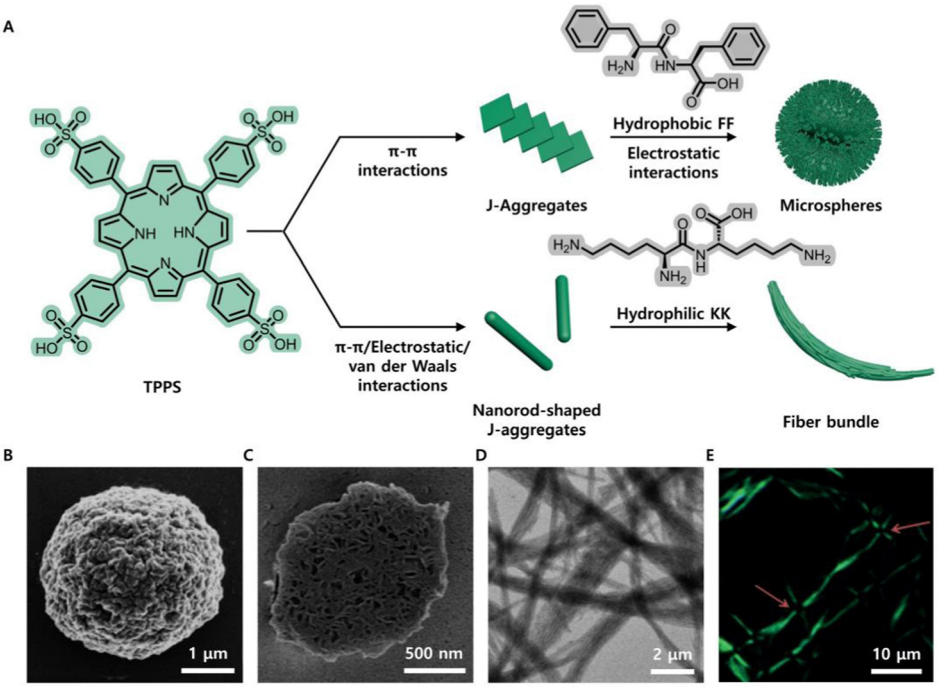

Fig. 2 (A) Schematic illustration of the fabrication of microspheres and fibre bundles by the coassembly of TPPS with amphiphilic FF and hydrophilic KK, respectively. (B) SEM image of the porphyrin-FF microsphere, showing irregular surface texture. (C) SEM image of the microsphere cross-section, showing a porous, multichambered interior. (D) TEM image of the porphyrin-KK bundled fibres. (E) Anisotropic photoluminescence at the intersection of orthogonal fibre bundles. Reproduced from ref. 48,49 with permission from [John Wiley and Sons], copyright [2014, 2015].

carboxylic groups, which facilitate amidation with the terminal amino group of the peptide and afford a new molecular chromophore–peptide conjugated compound (Fig. 3A).[21,39,50–53]

In the field of PDT, conjugating a photosensitizer (a tetrapyrrole compound, such as porphyrin and chlorin) to natural cationic antimicrobial peptides (such as buforin II, a 21 amino acid peptide, or magainin 2, a 23 amino acid peptide) results in the formation of a porphyrin–peptide conjugate with combined antimicrobial and PDT functions.[54,55] In addition to improving the solubility of hydrophobic photosensitizers, antimicrobial peptides also improve the PDT effect against different bacterial targets.[56] In addition, a *de novo* designed six-residue oligoarginine cationic peptide has been linked to a chlorin derivative (purpurin, P18) to selectively kill Gram-positive bacteria by inserting into the cell membrane, thus improving the photodynamic activity.[57] To improve the delivery of PDT for malignant tumours, cell-penetrating peptides (CPPs) have emerged as promising delivery agents for enhancing the cytosolic delivery. The short oligoarginine peptide sequence GRKKRRQRRRPPQ, which is derived from the human immunodeficient virus (HIV)-1 Tat protein residue 48–60, has been conjugated to hydrophobic porphyrins and chlorins to enhance their uptake in cancer cells.[58] In addition, Toddorovski *et al.* synthesized a series of peptide–porphyrin conjugates by coupling a porphyrin carboxyl group to an amino group (either the *N*-terminal or the Lys side chain) of the peptide shuttle, exhibiting an ability to cross the blood-brain barrier (BBB) and potential antiviral activities (Fig. 3B).[50]

The chromopeptide can also be designed to exhibit unique properties and complicated functions. Lu *et al.* used a fluorescence probe CREKA-Cy5.0 to determine the binding specificity of CREKA to the fibrin–fibronectin complexes in metastatic tumours (Fig. 3C).[59] Zheng *et al.* reported a stimulus-responsive molecular beacon composed of a pyropheophorbide (Pyro) and a singlet oxygen quencher motif which were covalently connected by a fibroblast activation protein (FAP)-responsive peptide.[60] The chromopeptide compound was intrinsically nontoxic due to the quenching of ROS. By FAP activation, the peptide is cleaved, and the remaining species turn to generate $^1O_2$ for cancer treatment. In a similar manner, Wang *et al.* designed a conjugate by combining P18, responsive peptide-sequenced YVHDC and CPP-sequenced GYGRKKRRQRRR (Fig. 3D).[61] It can be cleaved by caspase-1 and trigger assembly from monomer to aggregates. In addition, Kim *et al.* reported an internalizing cyclic peptide iRGDC-conjugated pyro derivative, which was further conjugated with quencher BK01 (pyropheophorbide-iRGDC-BK01).[62] The conjugate was designed as an *in situ* self-implantable photosensitizer. Its molecular functions include cancer cell internalization and photosensitization activated by tumour-selective proteolytic/reductive cleavage of the iRGD segment. Li *et al.* conjugated the cyclic pentapeptide cRGDfk and chlorin e6 (Ce6) to silk fibroin (SF) polypeptides.[63] SF acts as an integrator, which not only supports the photodynamic effect of Ce6 and the tumour targeting effect of cRGDfk but also improves the biocompatibility and biosafety of the chromopeptide materials. The above works show that the variations in each functional motif and its conjugation site are limitless; thus, the chromopeptide properties and applications may be constructed on-demand.

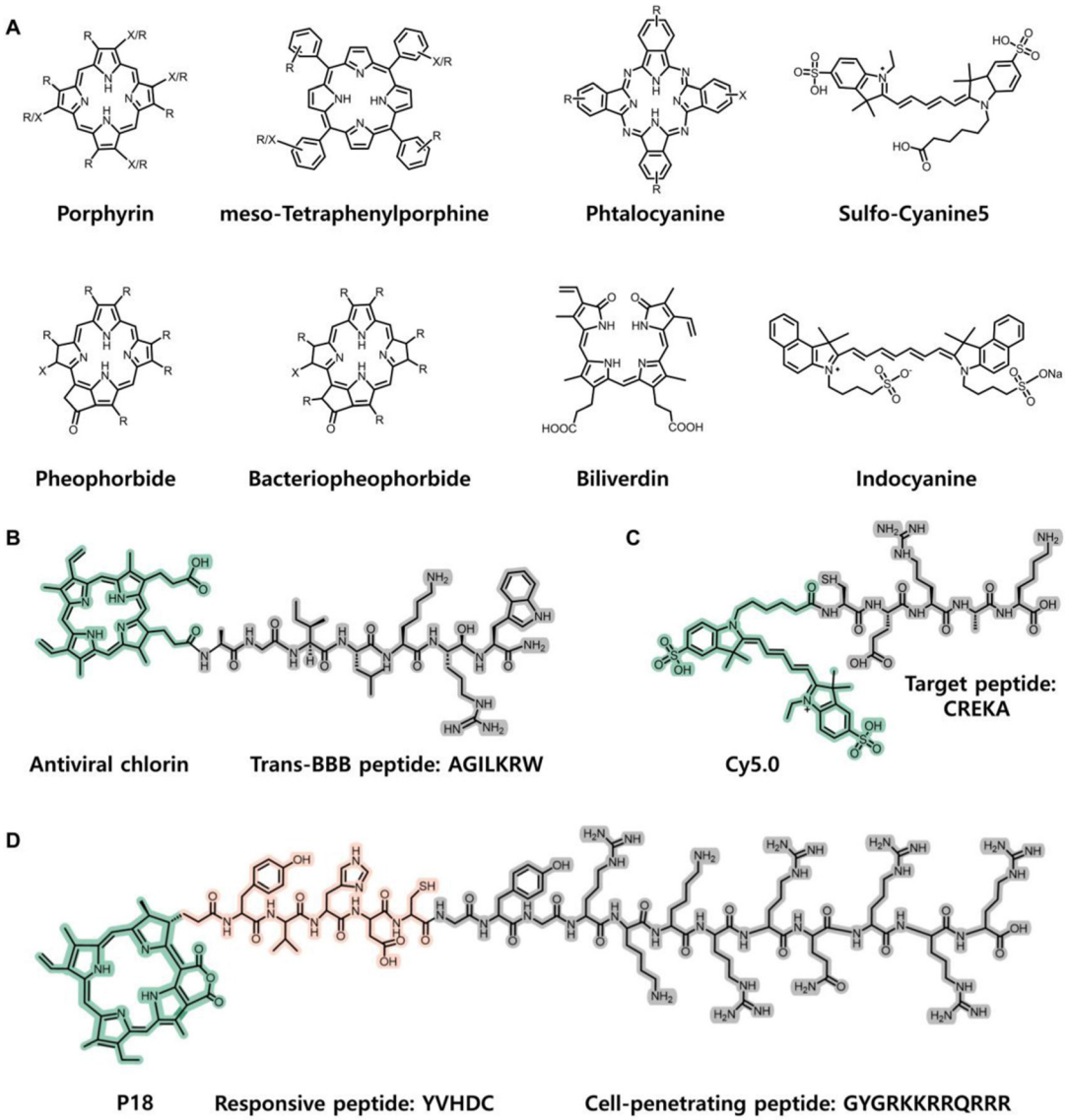

Fig. 3 (A) Basic structures of chromophores. ''R'' indicates an alkyl or alkenyl substituent, and ''X'' indicates the functional group for covalent linkage with the peptide chain. Reproduced from ref. 39 with permission from [John Wiley and Sons], copyright [2018]. Example structures of directly conjugated chromopeptides: (B) Chromopeptide directly conjugated between antiviral porphyrin and *trans*-BBB peptide AGILKRW. Reproduced from ref. 50 with permission from the [American Chemical Society], copyright [2021]. (C) Chromopeptide conjugated by Cy5.0 and target peptide CREKA. Reproduced from ref. 59 with permission from the [Nature Publishing Group], copyright [2015]. (D) Chromopeptide conjugated by P18, responsive peptide YVHDC and cell penetrating peptide GYGRKKRRQRRR. Reproduced from ref. 61 with permission from the [American Chemical Society], copyright [2016].

More interestingly, some natural photosensitizers and their derivatives contain more than one carboxylic group, and a great majority of peptide molecules contain multiple binding sites, which provides more abundant possibilities for modification and is advantageous for multifunctional molecular design.[64] Fernandez *et al.* conjugated two different chromophore molecules with dipeptide FF to obtain chromopeptide molecules *via* amidation. The two molecules exhibited the same one-dimensional nanofibre morphology under different assembly mechanisms.[65] Varying the protective group of the chromopeptide molecules or changing the external environment, such as the solvent, can produce assemblies with different structures. Coutsolelos *et al.* synthesized eight peptide–chromophore conjugates and assembled them by changing the solvent ratio to obtain adjustable sizes and structures, such as spiky spheres, nanofibres, hydrogels, and nanospheres.[66]

2.2.2 Conjugating chromopeptides with linkers or other chemical groups. In many cases, directly conjugating peptide motifs and chromophores *via* amidation does not support an easy synthesis process or functional applications of chromopeptide-based materials. As optimized strategies, these two parts may be conjugated or modified by external chemical groups. Introducing external chemical groups either tunes the assembling structures or optimizes the material functionality.

The additional linker functions as a spacer that separates the peptide motif and chromophore to an appropriatedistance

so that their respective functions are trivially affected by each other. 6-Aminohexanoic acid (Ahx) is an ω-amino acid with a hydrophobic and flexible structure and is a typical space linker that contains both terminal amino and carboxylic groups; in addition, a general solid phase peptide synthesis procedure similar to that of amino acids can be performed with Ahx.[67] For example, by inserting an Ahx residue between a cyclic 13-mer oligopeptide (Pep42, sequenced cyclic CTVALPGGYVRVC) and a fluoroalkyl zinc phthalocyanine, both the singlet oxygen ($^1O_2$) generation of phthalocyanine and the targeting ability toward the chaperone protein GRP78 of Pep42 were maintained.[68] Nevertheless, the bioconjugate is resistant to decomposition under $^1O_2$ generation. The zinc phthalocyanine-Ahx-Pep42 bioconjugates were designed to provide access to a new class of photoactive probes that can be useful for the rational development of catalytic materials. A similar effect was observed for a designed chlorin-type photosensitizer–peptide conjugate.[69] The researchers conjugated tetraphenylchlorrin (TPC) *via* a spacer (6-aminohexanoic acid, Ahx) to a vascular endothelial growth factor (VEGF) receptor-specific heptapeptide (ATWLPPR) (Fig. 4A). TPC was adopted as a model photosensitive chromophore that is easily available. TPC and ATWLPPR were coupled through the linker Ahx to achieve individualization. The photophysical properties of TPC remained unchanged after coupling with Ahx-ATWLPPR. In addition, the combination of ATWLPPR with Ahx does not affect the combination between the heptapeptide and neuropilin-1 (NRP-1). The presence of the Ahx spacer increased the flexibility of the molecule, and its length, and the nature of the molecule attached to it, impacted receptor affinity.

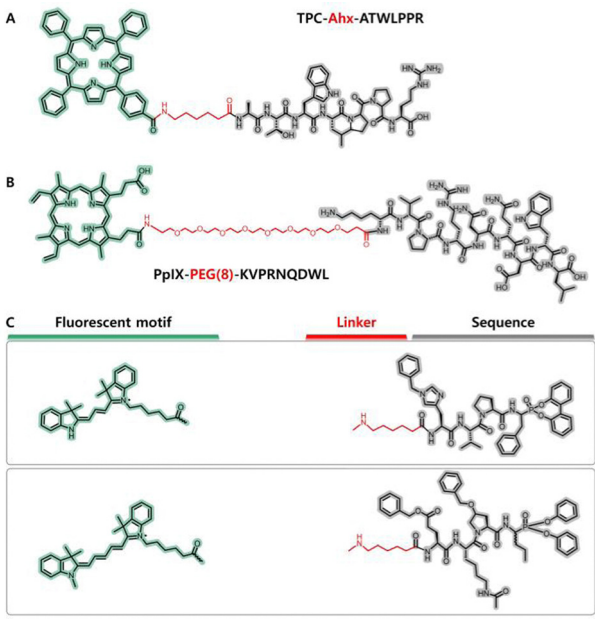

Fig. 4 (A) Molecular structure of a chromopeptide, namely, TPC–Ahx–ATWLPPR, in which an Ahx linker (marked with blue background) was employed for conjugation between a chlorin-type photosensitizer (TPC) and peptide motif. Reproduced from ref. 69 with permission from [Elsevier], copyright [2006]. (B) Molecular structure of another chromopeptide, namely, PpIX-PEG(8)-KVPRNQDWL, in which a PEG(8) linker (marked with blue background) was employed for conjugation between the PpIX motif and peptide motif. Reproduced from ref. 75 with permission from [John Wiley and Sons], copyright [2019]. (C) Representative structures of the motifs in the toolbox, including fluorescent motifs, linkers and specific sequences. Reproduced from ref. 77 with permission from the American Chemical Society, copyright [2017].

In addition to optimizing the distance between the peptide motifs and chromophores, the linker also provides a unique avenue for tuning the amphiphilicity of the conjugate. Polyethylene glycol (PEG) has been demonstrated to be a chemically inert, biocompatible and amphiphilic substance.[70,71] PEG that exhibits low degrees of polymerization and consists of a few periodic ethylene glycol units is a suitable candidate for coupling chromophores and peptide motifs for biological applications. Drag *et al.* designed a specific tetrapeptide sequenced Ac-Abu-DTyr-Leu-Gln-VS. for the main proteases of coronavirus disease 2019 (COVID-19) with an inhibition rate constant of $812 \pm 70\ M^{-1}\ s^{-1}$. To visualize the SARS-CoV main proteinase activity in patient samples, they further designed fluorescence activity-based probes (ABPs) that conjugate a dye to the tetrapeptide *via* a PEG(4) linker.[72] Due to the adequate length and amphiphilicity of PEG(4), the conjugate almost maintained its inhibitory activity with inhibition rate constants as high as $439 \pm 34\ M^{-1}\ s^{-1}$, and the detection sensitivity reached as low as 5 nM with a 2.5 μM conjugate solution.

In many cases, utilizing a PEG linker can realize the controllable construction of self-assembled nanostructures. It was reported that PEG chains have an important function of improving the circulation time of assemblies in blood, and connecting the assemblies with PEG can improve their stability.[73,74] Li *et al.* designed a self-delivery chimeric chromopepetide conjugate composed of a photosensitizer PpIX, a PEG(8) linker and a melanoma-specific antigen sequenced KVPRNQDWL (Fig. 4B).[75] The PpIX intrinsically has photodynamic activity under irradiation light and facilitates apoptosis and/or necrosis of melanoma cells with an intense immune response. This chromopeptide could self-assemble into spherical nanoparticles with an average size of 102 nm and a low polydispersity index of 0.197, which facilitated tumour accumulation through an enhanced penetration and retention (EPR) effect. A similar effect was found for the PpIX-PEG(8)-RDEVDG-K(TPE)-V-$CONH_2$ chromopeptide conjugate, in which TPE was a tetraphenylethylene derivative connected to the ε-amino group of Lys.[76] The conjugate with the PEG(8) linker exhibited a switchable morphology under different pH conditions. At pH = 7.4, the conjugate self-assembled into spherical nanoparticles, and under mildly acidic conditions, the conjugate exhibited a spherocylinder morphology.

Remarkably, the design of the linker depends on the chemical properties of each molecular motif and the intended function of the conjugate. However, it is not always easy to create an excellent design. Innovatively, researchers explored a toolbox for reliable parallel imaging of active neutrophil serine proteases, which contains a set of fluorescent probes, linkers and peptides (Fig. 4C).[77] The N-terminus contains fluorescent tags, and the linkers include PEG and Ahx. The researchers

attempted all possible combinations of motifs for each peptide specifically identifying NE, PR3, CATG or NSP4 in complex mixtures. As a result, highly selective chromopeptides that are responsive to different protein targets were screened. The amidation coupling described in the foregoing section shows limitations, that is, the carboxylic groups are necessary on both the chromophore motifs and the linkers, which may lead to tedious chemical modifications. In addition, an analogous method was applied to conjugate carboxyl-absent phthalocyanine with bioactive peptides, which have been successfully used as receptor-targeting bifunctional agents.[78]

With the burgeoning of ''click chemistry'', the conjugation between chromophores and peptides becomes more efficient and flexible.[79] The covalent bond formation can occur under mild conditions and be accurately controlled *in situ*. These methods of conjugating chromophores and peptide motifs remain under development. Prospectively, the relationship between molecular structures and self-assembled nanostructures together with their functions will be valuable to investigate.

3 Effects of intermolecular interactions on the assembly of chromopeptide

Intermolecular interactions are the underlying mechanism of self-assembly.[80–82] Representative intermolecular interactions include hydrogen-bonding interactions, electrostatic interactions (or Coulombic forces), hydrophobic interactions and van der Waals forces. The intensity and anisotropy of each interaction defined by a certain (combination of) molecule(s) lead to various self-assembled nanostructures. In fact, the method of peptide design has been utilized by many researchers to achieve the desired self-assembly nanostructures. There have been mature discussions on the assembly of peptides with diverse secondary structures. For example, peptides can be artificially designed as primary sequences and show the assembling tendency to certain supramolecular structures such as amyloids, hydrogels, and so forth, depending on the assembly properties of each amino acid residue and their integrated effects.[83] It is also true for those broadly studied peptide derivatives like lipopeptides and peptide–drug conjugates, where the modification group of linear alkyl chains provided hydrophobic interactions to the assembled system, and the assembly of drug molecular moieties was regulated by the conjugated peptide.[84,85] However, the situation becomes more complicated for the chromopeptide, as the chromophore exhibits a π-electron conjugated structure with intermolecular π–π interactions. These π–π interactions between chromopeptides are stronger and more anisotropic than those between individual peptides. Consequently, peptides bearing a chromophore show a more complicated self-assembly behaviour than that of chromophore-free peptide motifs.

A series of pH-sensitive self-assembling amphiphilic dye–cyclopeptide conjugated nanoprobes were designed.[86] The dye (CH1055) contained a fluorescent skeleton in the second near-infrared window (NIR-II) and was modified with a propionate group to reduce hydrophobicity. It was found that the size and structure of the assembly depend on the molecular design. When the dye and cyclopeptide were conjugated at a 1 : 1 molar ratio, CH-c(RGDfk) solid nanospheres were formed, and the size was approximately 80 nm. When the molar ratio was 1 : 3 (note that the dye contains four conjugatable branches), inhomogeneous CH-3c(RGDfk) nanovesicles were formed. Provided that the dye and the cyclopeptide were conjugated by a PEG(2) linker, size-reduced CH-PEG(2)-c(RGDfk) nanospheres with diameters of approximately 10 nm were formed. Clearly, the variance in these nanostructures is strictly related to the molecular structure of the chromopeptide.

Obtaining precise knowledge of the intermolecular interactions between chromopeptides is of paramount importance, and performing quantitative investigation on the contributions of intermolecular interactions is essential to control the self-assembled nanostructure and its functions in a more delicate way. Yan's group reported that FF-conjugated tetraphenylporphyrin (TPP-G-FF) could self-assemble into robust nanodots with a diameter of approximately 25 nm and excellent stability (Fig. 5A and B).[53] Molecular dynamics simulation revealed that the colloid stability resulted from the counterbalance between hydrogen-bonding interactions, which were contributed by the carboxyl group of peptides and solvent, as well as π–π interactions contributed by the porphyrins. Notably, individual FF is a self-assembled dipeptide that may afford various assembling structures depending on the assembly process,[87,88] while in contrast, the FF motif in TPP-G-FF played a role of inhibiting nanodot overassembly or overgrowth caused by the intense π–π interaction from the TPP motif, and providing aqueous stability for the nanodots (Fig. 5C). Such difference indicated that the π–π interactions between chromophore motifs were very strong and dominated the assembly. The overall effect of these interactions led to more complete fluorescence quenching of the nanodots compared to that of the TPP-FF monomeric solution; thus, the nanodots are an excellent candidate for a photothermal agent. Consequently, the photothermal conversion efficiency of the nanodots self-assembled by the peptide–porphyrin conjugate reached 54.2%, which is comparable to that of widely applied inorganic nanomaterials,[89,90] such as commercial Au nanoshells (13%) and nanorods (21%) and black phosphorus quantum dots (28.4%). Furthermore, Yan *et al.* proposed a new mechanism coined as ''supramolecular photothermal effects'', which is controlled by simple and flexible noncovalent intermolecular interactions for efficient thermal conversion.[91,92]

Recently, Yan *et al.* demonstrated that the intermolecular interactions, as well as the structural, energy-conversion, and therapeutic properties of supramolecular assemblies, can be customized by using amino acid-encoded peptide sequences.[93] The researchers selected pheophorbide A (PheoA), a natural chlorophyll derivative as the model chromophore because it absorbed far-red light strongly and had a carboxyl group available for coupling with peptides. Four oligopeptides sequenced as Asp (D), di-Asp (DD), FF, di-Tyr (YY) and tetraaspartic acid

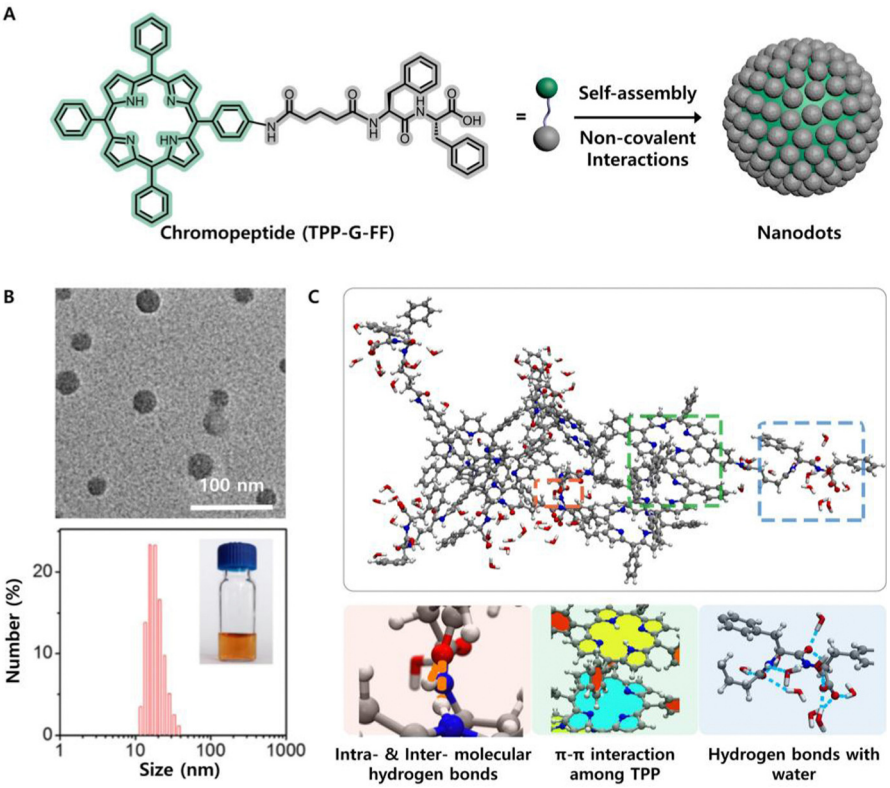

Fig. 5 (A) Schematic illustration of the self-assembly of a peptide–porphyrin conjugate (TPP-G-FF) into photothermal nanodots. (B) TEM image and DLS size distribution of the nanodots. The inset shows a picture of the nanodots in an aqueous solution. (C) Underlying intermolecular interaction mechanism of TPP-G-FF molecules obtained by MD simulation. Reproduced from ref. 53 with permission from the American Chemical Society, copyright [2017].

(DDDD), respectively, with distinct hydrophobicity were conjugated to PheoA to afford a chromopeptide building block. Remarkably, PheoA-FF self-assembled into nanoparticles, while the other conjugates self-assembled into nanofibrils. This is because FF is hydrophobic, while Y and D residues provide hydrophilic and anisotropic hydrogen-bonding interactions. All these nanoplatforms exhibited fluorescence quenching efficiencies higher than 85% and photothermal conversion efficiencies higher than 40%. The singlet oxygen quantum yields of the PheoA-D, PheoA-DD, PheoA-DDDD, PheoA-FF, and PheoA-YY nanoplatforms, in contrast, were distinguished by 0.214, 0.397, 0.494, 0.115, and 0.106, respectively. It seems that more hydrophilic nanofibres tended to exhibit higher singlet-oxygen quantum yields. In addition, these nanomaterials also exhibited different cellular internalization and disassembly behaviours in physiological environments. This study suggests that supramolecular assemblies based on chromopeptide conjugates with optimized phototherapeutic functions can be intentionally regulated by controlling noncovalent interactions through encoding the amino acid or peptide sequence.

4 Dynamically assembled nanostructures

Chromopeptide self-assembly is a strategy to produce desirable nanostructures and material properties by organizing designed molecular building blocks. Thermodynamics and kinetics of peptide self-assembly play key roles in structural modulation and function integration.[33] Since the chromopeptide building blocks can be flexibly designed and their assembly process can be precisely controlled, the resulting assembled structures and functions are diverse and fascinating. This section focuses on how to modulate the nanostructures and functions of chromopeptide assemblies.

The thermodynamic and kinetic conditions, including solvent, concentration, spaciotemporal variance in species, temperature, and so forth, are external environments that strongly affect the chromopeptide self-assembly process as well as the nanostructures and their functionality.

Self-assembled chromopeptide materials have a wide range of biological applications, mainly in physiological settings. Therefore, pH is among the most important thermodynamic parameters. Utilizing the pH difference between normal tissue (pH $\approx$ 7.4) and the tumour region (pH $<$ 6.5), a self-transformable pH-driven chromopeptide (PpIX-AEQNPIYWARYADWLFTT-PLLLLDLALLVDADEGT, a conjugate of protoporphyrin and a membrane-anchoring peptide) was designed.[94] The peptide is pH-responsive; thus, the chromopeptide remained monomeric due to hydrophilicity at pH $\approx$ 7.4, while the peptide motif turned into an α-helical structure and inserted into the cell membrane after the pH was reduced to 6.5. The pH-triggering dynamics of the chromopeptide facilitated the *in situ* generation of ROS upon light irradiation and direct damage to tumour membranes.

Notably, the thermodynamic conditions are highly related to self-assembly kinetics and lead to complexity in the self-assembly pathway. Therefore, a chromopeptide building block may self-organize into more than one kind of assembly depending on the thermodynamic and kinetic conditions. Yan and co-workers prepared a model chromopeptide molecule, FF-conjugated phthalocyanine (PF, Fig. 6A), in which phthalocyanine is an excellent self-assembling unit due to its highly symmetrical structure and unique intermolecular π–π interactions. The model building block, PF, could self-assemble into nanoparticles by rapid precipitation; specifically, a very small amount of DMSO solution of PF was simply titrated into water. However, by increasing the ratio between DMSO and water and titrating the DMSO solution of PF into water repeatedly over 72 h, a new self-assembly morphology was obtained rather than nanoparticles (Fig. 6B).[95,96] The new morphology was helical nanofibrils, which exhibited a greater thermodynamic stability than that of nanoparticles. Compared with the PF monomer and nanoparticles, more interestingly, the nanofibrils exhibited a very large redshifted absorption (105 nm) and moved to the NIR region (Fig. 6C). The variance in self-assembled nanostructures occurred because rapid precipitation is an entropy-dominated process and the molecules are isotropically assembled. In contrast, the slow and fractional titration allows the molecules to find a thermodynamically favoured supramolecular structure and is an enthalpy-dominated process. Due to the closely stacked phthalocyanine motifs that contain unique π–π interactions between them, the absorption spectroscopy also drastically changes (Fig. 6D). This pathway-selective self-assembly provides more possibilities for the functionalization of chromopeptide materials.

The kinetic control of chromopeptide self-assembly can be accompanied by stimulus-triggered chemical reactions. In this way, the nanostructures and functions of nanomaterials exhibit dynamic variation depending on the external environment. For example, a P18-peptide (sequenced PLGVRGRGD) was designed for cancer diagnostics and phototherapy.[97] The chromopeptide diffused in the physiological environment and targeted $\alpha_v\beta_3$ integrins due to the presence of the terminal RGD ligand. Furthermore, the PLGVRG motif is enzyme responsive and can be cleaved by the overexpression of gelatinase in the tumour microenvironment, causing the chromopeptide to decompose. Consequently, the chromopeptide simultaneously self-assembled into nanofibres at tumour sites, exhibiting an assembly induced retention (AIR) effect, which resulted in an improved imaging signal and enhanced phototherapeutic efficacy.

The coupling between self-assembly and enzyme-responsive reactions usually renders a cascaded synergistic effect. A chimeric chromopeptide C16-K(PpIX)-PEG(8)-KDEVD-1MT (PpIX-1MT) was designed, in which C16 is a hydrophobic palmitoyl group, the photosensitizer PpIX is conjugated to the ε-amino group of Lys, DEVD is a caspase-3-sensitive peptide sequence, and 1MT refers to 1-methyltryptophan.[98] The chromopeptide PpIX-1MT could initially form nanoparticles in phosphate buffer solution (PBS) and accumulate in tumour regions; then, reactive oxygen species (ROS) are produced and 1MT is released upon caspase-3 cleavage, which triggers an intense immune response. Similarly, a tumour

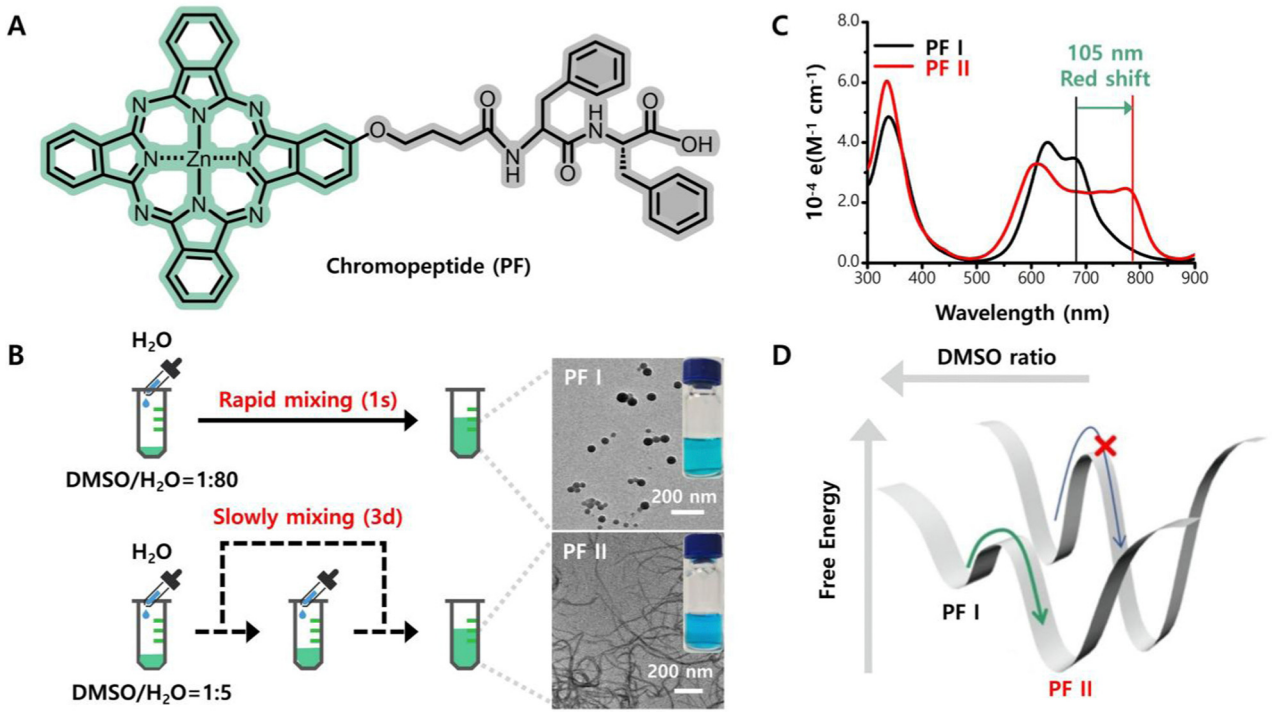

Fig. 6 Kinetically controlled self-assembly of phthalocyanine–diphenylalanine (PF) enables a very large redshifted absorption. (A) Molecular structure of chromopeptide PF. (B) Schematic illustration of two assembly processes and the resulting assembly morphologies. (C) Electronic absorption spectra of the two assemblies. (D) Underlying thermodynamics of PF assemblies. Reproduced from ref. 95,96 with permission from the [Chinese Chemical Society], copyright [2019, 2021].

extracellular acidity-responsive conjugated chromopeptide PpIX-Ahx-AEAEAKAKAEAEAKAK (PEAK) was designed, in which the ε-amino group of each Lys residue was initially protected by an acid-labile dimethylmaleic anhydride (DMA) group.[99] PEAK underwent self-assembly into stable nanoparticles, which was driven by the synergistic effect of ionic complementarity (a special kind of electrostatic interaction), hydrogen-bonding interactions, van der Waals forces and hydrophobic interactions. Comparably, in a tumour environment with a low pH, the DMA groups were cleaved, baring the positively charged amino group. Due to the enhanced ionic complementarity, the nanoparticles transformed into nanorods, which facilitated the internalization of tumours, thus achieving improved phototherapeutic efficacy. Remarkably, chromopeptide design with dynamic and tunable self-assembly ability provides opportunities to realize complicated functions.

5 Applications

Self-assembled chromopeptide systems offer unique advantages for biological applications. As a key component of chromopeptides, peptide motifs exhibit good biocompatibility, biodegradability, programmability and diverse biological functionalities. Chromophores with tunable optical properties offer multiple opportunities in diagnosis, therapy, energy conversion, *etc.* Utilizing bioactive peptides may greatly expand the functionality of self-assembled chromopeptide systems. In addition, assembling chromopeptides offers a solution for inhibiting the enzymatic degradation and rapid metabolism of chromopeptides in the biological environment. Thus, based on the knowledge of the self-assembly mechanism detailed above, self-assembled chromopeptide systems may be promising candidates for bioimaging, phototherapy, combined therapy, biomimetic photocatalysis and photosynthesis.

5.1 Imaging

Similar to chromoproteins, chromopeptides play an important role as powerful imaging tools. Some chromopeptides perform imaging functions that can be used as guidance tools for optical biopsy to specifically illuminate malignant disease areas. For example, BLZ-100 is a chromopeptide that contains a chlorotoxin peptide (36-amino acid peptide)[100,101] and the NIR fluorescence imaging molecule indocyanine green (ICG) can specifically label solid tumour tissue and emit fluorescence in the NIR range for intraoperative visualization of human tumours. Importantly, chromopeptides can then self-assemble into supramolecular nanostructures with imaging capabilities (Table 1). This subsection summarizes chromopeptide nanomaterials applied for bioimaging.

Chromopeptide nanomaterials disassemble to emit fluorescence signals after reaching the target site *in vivo* over time, so these materials can potentially be used as bioimaging agents for cell imaging and *in vivo* fluorescence imaging (FLI). This is mainly because the excited pigment molecules in the chromopeptide system release energy through fluorescence emission and return to the ground state. Yan *et al.* utilized the hydrophobic and π–π stacking interactions between a cationic diphenylalanine (CDP) derived from FF and hydrophobic photosensitive Ce6 to self-assemble into chromopeptide spherical nanoparticles (CCNPs).[19] The self-assembled chromopeptide nanospheres were taken up by MCF-7 cells and decomposed over time to release fluorescent signals, thereby realizing FLI of cells *in vitro* and dynamic fluorescence distribution in mice *in vivo*. Compared with the molecular state of photosensitive Ce6, chromopeptide nanoassemblies show enhanced structural stability, thus achieving longer imaging sessions *in vivo*. When the peptide motif of the chromopeptide is endowed with specific biological activity, controllable intelligent imaging becomes a reality. For example, a chromopeptide conjugate was designed, which

Table 1 Summary of chromopeptide assemblies for imaging

Chromopeptide-based nanomaterials	Chromophore	Peptide	Morphology	Application	Ref.
CCNPs	Ce6	CDP	Nanoparticles	FLI	19
TCASS	Cy	AVPIAQKDEVDKLVFFAECG	Nanofibres	FLI	102
ZB NPs	BV	His-containing	Nanoparticles	PAI	103
ZBMn NPs	BV	His-containing	Nanoparticles	PAI/MRI	
P18-PLG	P18	PLGVRG	Nanofibres	PAI	97
PD-NFs	PheoA	D	Nanofibres	PAI	93
PDD-NFs	PheoA	DD	Nanofibres	—	
PFF-NPs	PheoA	FF	Nanoparticles	—	
PYY-NFs	PheoA	YY	Nanofibres	PAI	
PDDDD-NFs	PheoA	DDDD	Nanofibres	—	
PWG	Porphyrin	WG	Nanoparticles	FLI	104
TP5-ICG NFs	ICG	TP5	Nanofibres	PAI	105
ZnPc-GGK(B)COOH NP	ZnPc	GGK(B)-COOH	Nanoparticles	FLI	106
ZnPc-GGK(B)$CONH_2$ NP	ZnPc	GGK(B)-$CONH_2$	Nanoparticles	FLI	
PPP-NDs	Porphyrin	FF	Nanodots	PAI	53
PF NPs	ZnPc	FF	Nanoparticles	FLI/PAI	107
PEAK-DMA	PpIX	AEAEAKAKAEAEAKAK	Nanoparticles	FLI	99
ACPP-PpIX	PpIX	R9GPLGLAGE8	—	FLI	108
PPF	Pyro	GDEVDGSGK	—	FLI	109
ELP-IR820	IR820	Elastin-like polypeptides (ELPs)	Nanoparticles	—	110
MRI	ICG	RADA32−melittin	Hydrogel	FLI/PAI	111

"—" represents "Not provided".

consisted of a tumour-specific recognition motif (sequenced AVPIAQK), an enzymatic cleavage linker (sequenced DEVD), a self-assembly motif (sequenced KLVFFAECG) and a cyanine dye Cy.[102] Under the action of the tumour recognition motif, chromopeptide molecules entered tumour cells and were cleaved by caspase-3/7 to trigger self-assembly *in vivo*, while the remaining residues self-assembled into β-sheet nanofibres under the action of hydrogen bonds. Due to the significant permeability of chromopeptide molecules, these self-assembled nanofibres *in vivo* exhibited high cumulative efficiency, and the fluorescent signals used for *ex vivo* imaging of intact patient bladders exhibited high specificity and sensitivity, which had an important clinical value in image-guided surgery for bladder cancer.

In addition, chromopeptide nanomaterials are also applied in photoacoustic imaging (PAI), a nonionizing imaging modality based on the photoacoustic (PA) effect,[112–114] which depends on the physiochemical properties of the chromophore segment. Yan *et al.* constructed a series of supramolecular assemblies based on well-designed chromopeptides. For example, the researchers designed nanoparticles with broad NIR absorption using the endogenic biopigment biliverdin (BV) and a His-containing peptide (*Z*-His-Obzl, ZHO), which can be used as PAI contrast agents for diagnosing tumours with high spatial resolution and penetration depth.[103] More importantly, the metal ion Mn^{2+} was integrated into the chromopeptide nanoparticles, which enhanced the photostability of the nanoparticles and endowed the nanoparticles with magnetic resonance imaging (MRI) capabilities. Dual-modal imaging, which integrates PAI and MRI, offers precise imaging guidance for photothermal therapy (PTT) of tumours. Chromopeptide assemblies are widely used in FLI and PAI because they contain natural chromophores. In addition, chomopeptide assemblies are also considered to have great potential in other imaging fields. On the one hand, the assemblies can be used as a carrier of other imaging agents; on the other hand, the assemblies with other imaging capabilities such as ultrasound imaging can be obtained by designing the molecular structure of chromopeptides. However, it still requires researchers to explore the application of chromopeptide assemblies much more in the imaging field.

5.2 Phototherapy

Phototherapy is a clinically approved technique that involves treating diseases with a laser, which is used as a scalpel.[115–118] Compared with conventional therapeutic methods, phototherapy exhibits several advantages, including minimal invasiveness, convenient operation, fast recovery and strong specificity. For phototherapeutic purposes, the chromophore plays a key role in converting light energy to reactive oxidative species (ROS, for PDT, Section 5.2.1) or to local tumour hyperthermia (for photothermal therapy, Section 5.2.2), which leads to disease suppression under different mechanisms. The photoconversion mechanism depends on both the intrinsic physiochemical properties of the chromophore and the supramolecular structure of the chromopeptide assemblies. Coincidentally, the peptide motifs in the chromopeptide system interact with chromophores to form assembled materials with different structures and flexible functions, providing the possibility to tune the physical and chemical properties of phototherapeutic agents (Table 2); thus, the system exhibits high potential for phototherapy applications.

5.2.1 Photodynamic therapy. Chromopeptide assemblies can be used for PDT due to their enhanced photochemical stability along with their improved safety as photochemical sensitizers. PDT is a photochemical reaction process in which the photosensitive chromophore returns from the excited state to the ground state under laser irradiation to produce ROS and kills the diseased tissue.[132] In this method, the chromophore motif must involve a large yield of singlet oxygen, considerable stability, biocompatibility and degradability. Effective PDT can be realized through the molecular design of chromopeptide motifs and by regulating the assembly process.

5.2.1.1 Photodynamic antitumour therapy. Chromopeptide assemblies can effectively treat tumours in terms of the PDT effect. Inspired by the multicomponent self-organization of natural proteins, pigments and metal ions in metalloproteins,[133–136] Yan *et al.* chose metal-binding amino acids or peptides, photosensitizer Ce6 and metal ions Zn^{2+} to construct multicomponent coordination chromopeptide-based assemblies (Fig. 7A).[137] Metal coordination is a directional and reversible chemical bond, and its bonding strength is stronger than that of noncovalent interactions.[138,139] Therefore, the chromopeptide-based assemblies formed by metal coordination show strong colloidal stability, which is not exhibited by those formed through nonmetal coordination. More importantly, the assemblies showed that the photosensitizers exhibited a capacity for ultrasensitive pH-responsive release. This is closely related to metal coordination. The protonation of the imidazole group at pH values below 5.0 effectively weakens the coordination between His and Zn^{2+}. The sensitive response to the pH increase can be attributed to the improved solubility of His-containing amino acids or peptides at pH values above 8.5, which diminished the self-assembly hydrophobic interactions. In addition, since the coordination inhibited intramolecular motion, the emission path of Ce6 was effectively enhanced, and the nonradiative heat release path was suppressed, showing high ROS yield *in vitro* (Fig. 7B) and highly efficient PDT *in vivo* (Fig. 7C and D). By purposefully designing chromopeptides, mimicking the composition of metalloproteins, and utilizing a coordinated self-assembly approach, it is possible to successfully combine robust blood circulation and targeted burst release into a single chromopeptide system for efficient photodynamic cancer treatment.

In many cases, the photodynamic therapeutic efficacy is remarkably influenced by the nanoparticle morphology. Inspired by the dynamic changes in the morphology of molecular assemblies in organisms to complete different life processes, van Hest *et al.* prepared pH-responsive transformable chromopeptide-based nanomaterials using Try–Gly–porphyrin conjugates (PWG) as the assembly motif.[104] These nanomaterials appeared like a nanoparticle under neutral conditions. Comparably, when exposed to acidic conditions, such as the tumour microenvironment, the nanoparticles converted into

Table 2 Summary of chromopeptide assemblies for applications in phototherapy and combinational phototherapy

Chromopeptide-based nanomaterials	Chromophore	Peptide	Morphology	Application	Ref.
CCNPs	Ce6	CDP	Nanoparticles	PDT	19
ZB NPs	BV	His-containing	Nanoparticles	PTT	103
ZBMn NPs	BV	His-containing	Nanoparticles	PTT	
P18-PLGVRGRGD	P18	PLGVRGRGD	Nanofibres	Targeted therapy combined with PTT	97
PD-NFs	PheoA	D	Nanofibres	PTT	93
PDD-NFs	PheoA	DD	Nanofibres	—	
PFF-NPs	PheoA	FF	Nanoparticles	—	
PYY-NFs	PheoA	YY	Nanofibres	PTT	
PDDDD-NFs	PheoA	DDDD	Nanofibres	—	
PWG	Porphyrin	WG	Nanoparticles	PDT	104
TP5-ICG NFs	ICG	TP5	Nanofibres	Immunotherapy combined with PTT	105
ZnPc-GGK(B)COOH NP	ZnPc	GGK(B)-COOH	Nanoparticles	Chemotherapy combined with PDT	106
ZnPc-GGK(B)$CONH_2$ NP	ZnPc	GGK(B)-$CONH_2$	Nanoparticles	Chemotherapy combined with PDT	
PPP-NDs	Porphyrin	FF	Nanodots	PTT	53
PF NPs	ZnPc	FF	Nanoparticles	PDT and PTT	107
PEAK-DMA	PpIX	AEAEAKAKAEAEAKAK	Nanoparticles	PDT	99
ACPP-PpIX	PpIX	R_9GPLGLAGE$_8$	—	PDT	108
PPF	Pyro	GDEVDGSGK	—	PDT	109
ELP-IR820	IR820	Elastin-like polypeptides (ELPs)	Nanoparticles	PTT	110
MRI	ICG	RADA32−melittin	Hydrogel	PTT	111
Pep@Ce6	Ce6	Cationic polypeptide	Spherical micelles	PDT	119
APP	Ce6	GKRWWKWWRRPLGVRGC	—	PDT	120
ELTST	Ppa	GPLGLAG	Nanovesicles	Chemotherapy combined with PDT	121
Ce6-DEVD-MMAE	Ce6	DEVD	Nanoparticles	Chemotherapy combined with PDT	122
MEL/Ce6@HA	Ce6	Melittin	Nanoparticles	Chemotherapy combined with PDT	123
PAPP-DMA	PpIX	PKKKRKV	Nanoparticles	Targeted therapy combined with PDT	124
UCNPs@TiO_2-Ce6-TAT	Ce6	TAT	Core/shell	Targeted therapy combined with PDT	125
pnPNP	PpIX	PKKKRKV	Nanorods	Targeted therapy combined with PDT	126
M-ChiP	PpIX	rFxrFxrFxr	Spherical micelles	Targeted therapy combined with PDT	127
HB-PA	HB	CRGDKGPDC	Nanovesicles	Targeted therapy combined with PDT	128
Ppa-iRGDC-BK01	Ppa	iRGDC	—	Targeted therapy combined with PDT	62
ChiP-Exo	PpIX	PKKKRKV	Exosomes	Targeted therapy combined with PDT	129
TPC-Ahx-ATWLPPR	TPC	ATWLPPR	—	Targeted therapy combined with PDT	69
ZnPc-BBN	ZnPc	YQRLGNWAVGHLM	—	Targeted therapy combined with PDT	78
RGD-L-Pyro	Pyro	cRGDfK	—	Targeted therapy combined with PDT	130
RGD-L-Glu-Pyro	Pyro	cRGDfK	—	Targeted therapy combined with PDT	
PPMA	PpIX	KVPRNQDWL	Nanoparticles	Immunotherapy combined with PDT	75
PpIX-1MT	PpIX	KDEVD	Nanoparticles	Immunotherapy combined with PDT	98
mPEG-Pep-IDOi/ICG	ICG	PVGLIG	Core–shell	Immunotherapy combined with PTT	131
IR780-M-APP	IR780	NYSKPTDRQYHF-NH_2	Nanoparticles	Immunotherapy combined with PDT	132

"r" represents d-Arg and "Fx" represents l-cyclohexylalanine; "—" represents "Not provided".

nanofibres, which was mainly because the protonation of PWG promoted the formation of intermolecular hydrogen bonds. These chromopeptide nanofibres enhanced intersystem crossing through fibrillar transformation to promote the generation of singlet oxygen, realized the effective accumulation and long-term retention of photosensitive drugs at the tumour site, and thus exhibited excellent antitumour therapeutic effects *in vivo*. Surprisingly, researchers used PpIX and low pH insertion peptides (pHLIP) to design a chromopeptide self-assembled material with an ability to anchor membranes through pH-driven secondary structure transformation, which was not affected by tumour heterogeneity.[94] Specifically, the material showed a structural transition from random coils at pH 7.4 to α-helices at pH 6.5 or 5.5 through the action of pHLIP; thus, the material can spontaneously insert into the lipid bilayer without cell internalization to achieve tumour-specific accumulation and realize *in situ* PDT on the cell membrane. In addition, Yu *et al.* developed tumour microenvironment-adaptable chromopeptide-based superhelices and nanoparticles by coassembling pentapeptide FF-Amp-FF (AmpF) with Ce6.[140] The adaptation occurred because the 4-amino-proline amide bond in AmpF was *trans*-isomerized at a low pH (6.5) and *cis*-isomerized at a high pH (7.2). More importantly, compared with nanoparticles, nanofibres formed by reversible transformation of nanoparticles in the cytoplasm produced higher levels of ROS, so the therapeutic effect could be maintained even with a reduction in dosage. Although the chromopeptide assemblies used for anti-tumour have increased intelligence, most of them are based on the passive transport of nanomaterials, which requires nanomaterials to have strong structural stability. In addition, the active targeting of the lesion needs to be strengthened, especially the chromopeptide assemblies applied in photodynamic therapy of cancer.

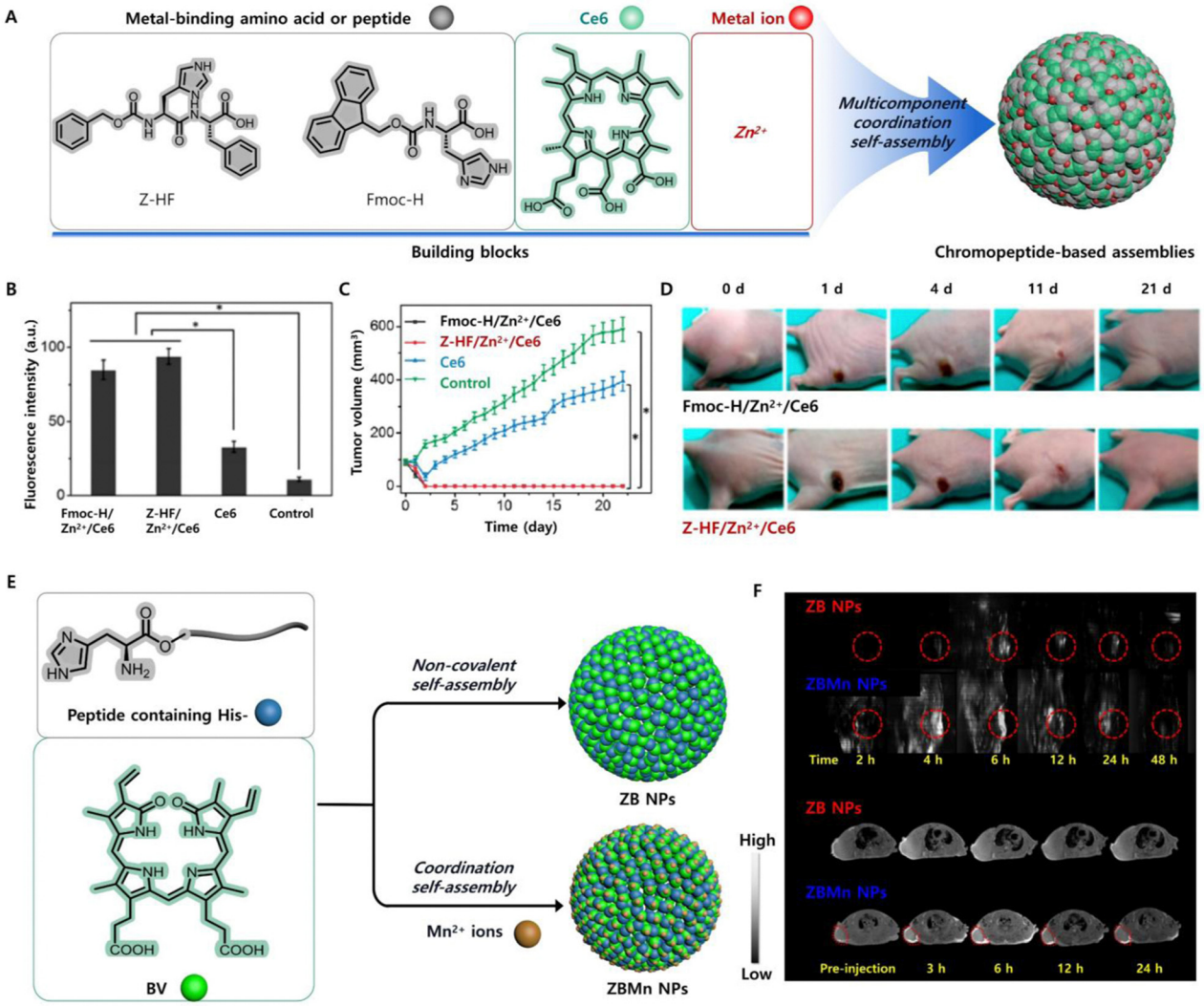

Fig. 7 (A) Schematic illustration of a chromopeptide system formed by multicomponent self-assembly. (B) Fluorescence intensity of cells, showing the ROS produced by different groups of drugs after irradiation. (C) Tumour growth profiles during the observation *in vivo*. (D) Photographs of all mice or tumours in different groups after treatment *in vivo*. Reproduced from ref. 137 with permission from the [American Chemical Society], copyright [2018]. (E) Schematic illustration of the formation of chromopeptide-based nanoparticles. (F) PAI (upper) and (below) T_1-weighted MRI of chromopeptide-based nanoparticles in mice. Reproduced from ref. 103 with permission from [John Wiley and Sons], copyright [2019].

5.2.1.2 Photodynamic antibacterial therapy. Chromopeptide assemblies are not only used in photodynamic anti-tumour therapy, but also used in antibacterial therapy. PDT for bacterial infection has attracted great attention because it has the advantage of rare drug resistance, but it is also limited by the short life of ROS and the poor sensitivity to Gram-negative bacteria. The researchers used chlorin e6 (Ce6)-conjugated α-cyclodextrin (α-CD) and a polyethylene glycol (PEG)ylated polypeptide (Pep) as assembly units to obtain chromopeptide-based micelles (Pep@Ce6), which showed good therapeutic effects in bacterial infections caused by Gram-negative bacteria.[119] This was because cationic chromopeptide-based micelles had enhanced bacterial membrane capture ability, and could effectively play a photodynamic role in eliminating biofilms and inactivate persistent cells.

In addition, *Staphylococcus aureus* infection is also the most common type of bacterial infection, and the increase in drug resistance is also a major threat to the treatment of these infections. Xia and other workers designed a chromopeptide based on the covalent coupling of Ce6 with the polycationic antimicrobial peptide (GKRWWKWRR) modified by the gelatinase cutting peptide sequence (PLGVRG).[141] The chromopeptide could eliminate bacterial infection and inhibit the formation of bacterial biofilms *in vitro* under laser irradiation. When Ce6 was coupled with dimer peptides, the wound healing speed and quality of mice infected with *Staphylococcus aureus* were also improved. More importantly, they found that after assembling the chromopeptide with gold nanoclusters (AuNc), a synergistic effect between gelatinase responsive release of chromopeptides and photodynamic therapy was achieved.[120] Because the gelatinase secreted by *Staphylococcus aureus* effectively promoted the release of chromopeptide molecules containing antibacterial peptides from AuNc, the therapeutic effect of *Staphylococcus*

aureus was superior to that of *Escherichia coli*. The chromopeptide assemblies are expected to provide guidance for the development of materials for the treatment of bacterial infection and the promotion of wound healing. At present, many chromopeptides have been designed, but whether they can be assembled and how they can be released at specific lesion sites after assembly need further study. In addition, some research studies has found that the peptide itself has antibacterial activity,[142,143] which greatly promotes the application of chromopeptides in antibacterial therapy.

5.2.2 Photothermal therapy. Many chromopeptide assemblies can convert photoenergy into heat energy through a thermal release mechanism to ablate diseased tissues or tumours, so these assemblies are also used in cancer photothermal therapy (PTT).[144–146] Compared with PDT, PTT exhibits several advantages, as it is not limited by oxygen and releases heat through nonradiative vibrational relaxation pathways. Therefore, how to regulate the photosensitive chromophore molecules in the chromopeptide system to release more heat is a challenge in effective photothermal therapy.

Inspired by light-absorbing haemoglobin photothermal biological macromolecules, Yan *et al.* proposed a method for the self-assembly of chromopeptide conjugates to prepare nanodots for photothermal antitumour therapy.[53] Chromopeptide conjugates (TPP-G-FF) were formed by connecting FF and porphyrin with glutaric anhydride as a linker. These conjugates self-assembled in water to produce nanodots with a uniform distribution. The formation mechanism of chromopeptide nanodots was studied by molecular dynamics simulation, and the results showed that TPP tended to form J-aggregates due to π–π interactions, and the strong hydrophilic interaction between FF and solvent was beneficial for increasing the nanodot stability. Therefore, the fluorescence emission path and singlet oxygen generation path of the chromopeptide-based nanodots are nearly suppressed, so the photoenergy tends to be converted to the local high temperature. Hence, chromopeptide-based nanodots can achieve more efficient photothermal transformation, generate higher local temperatures and enhance antitumour effects and can also be used as ideal PAI agents. However, although the chromopeptide-based nanodots greatly improved the stability, there were still problems, *i.e.*, an insufficient absorption wavelength and insufficient laser penetration. Specifically, Yan and co-workers assembled chromophore BV and peptide motif ZHO into chromopeptide-based nanoparticles (ZB NPs) with NIR broadband wavelength absorption through noncovalent interactions.[103] ZBMn NPs were obtained by integrating Mn^{2+} into ZB NPs to further improve the stability and MRI capabilities (Fig. 7E). As expected, the obtained ZBMn NPs broadened the absorption spectrum to a longer NIR region and exhibited efficient photothermal conversion. Moreover, compared with nanoparticles without metal ions, ZBMn NPs exhibited excellent stability after illumination, mainly due to the coordination of metal ions and peptide chain imidazoles. PAI and MRI showed that the maximum accumulation of nanoparticles at the tumour site occurred 6 h after tail vein administration (Fig. 7F). These chromopeptide-based nanoparticles utilize a clear metabolic mechanism, which provides the possibility for clinically transforming chromopeptide-based nanoparticles to photothermal agents under the guidance of multimodal imaging. The PTT effect of ZBMn NPs was verified in mice. The results showed that the tumours were ablated without recurrence in the PTT group during the whole observation period, while the tumour volume of the control group increased rapidly over time. The tumour photographs recorded over time clearly showed that after photothermal treatment with ZBMn NPs, the tumour first scabbed and then slowly fell off without recurrence.

Chromopeptide photothermal agents have shown advantages for solving the poor penetration and low accumulation efficiency of nanomaterials at tumour sites. For example, Wang *et al.* developed a molecular-level deep tissue penetration and NIR laser-guided *in situ* self-assembly strategy, which greatly improved the penetration depth and accumulation of nanomaterials at tumour sites.[147] This was achieved by integrating a thermally responsive scaffold (poly(β-thioester)) into a chromopeptide system that contained the photothermal molecule ICG and functional peptides (cytotoxic and cell penetrating peptides). Specifically, the obtained molecular-level substances reached the interior of the tumour at normal body temperature and generated heat under laser irradiation, resulting in thermoresponsive *in situ* self-assembly into spherical nanoparticles, which was beneficial for intratumoral aggregation and cell killing. Given the *in situ* self-assembly effect of chromopeptides under NIR laser irradiation, many other drugs with high anticancer activity can be integrated into the chromopeptides to achieve enhanced antitumour effects. In addition, Yan *et al.* designed five chromopeptide conjugates by encoding peptide sequences with amino acids, which can self-assemble into assemblies with different optical properties.[93] By regulating the self-assembly process, assemblies with a stable structure and excellent photothermal performance were finally optimized, and the tumours in mice were successfully eliminated. PTT can ablate tumour lesions, and in antibacterial therapy, there are also some reports of using inorganic photothermal materials to resist bacteria.[148] However, few chromopeptide assemblies are used for photothermal antibacterial therapy. It is believed that with the attention paid to chromopeptides, chromopeptide assemblies will also have rapid development in photothermal antibacterial and other biomedical fields.

5.3 Combinational phototherapy

A combination of phototherapy and other theranostic methods may lead to synergistic effects, which will be a future trend in cancer therapeutics. The combined methods mainly include chemotherapy, targeted therapy, immunotherapy and other therapies. For combinational phototherapeutic purposes, it is necessary to design chromopeptides more precisely and ingeniously and endow them with multiple functions.

5.3.1 Chemotherapy combined phototherapy. Chemotherapy, which is among the most traditional methods of treating cancer, works through chemical drugs that exhibit killing effects.[149] However, due to a lack of selectivity, chemotherapeutic drugs cannot reach and accumulate at the tumour site; thus, these drugs cause large toxic side effects on normal tissues.[150,151]

In addition to exhibiting phototherapeutic activity, chromopeptide assemblies can be used to carry chemotherapeutic drugs; thus, these assemblies realize the combination of phototherapy and chemotherapy and improve the efficacy and safety of tumour treatment to a certain extent. A chromopeptide-based material with a programmed stimuli-responsive liposomal vesicle structure was reported, and this material could be loaded with a lipophilic oxaliplatin prodrug of hexadecyloxaliplatin carboxylic acid (HOC) and hydrophilic doxorubicin hydrochloride (DOX) (Fig. 8A).[121] Chromopeptide nanovesicle structures (LTSL) consisted of a photoresponsive PPa, a GPLGLAG heptapeptide spacer, a PEG chain and a temperature-sensitive liposome (TSL). Drug-loaded nanovesicles (ELTSL) accumulated at tumour sites through the enhanced permeability and retention (EPR) effect, PEG antennae were cleaved by intratumoral matrix metalloproteinase 2 (MMP-2), and the remaining components could be internalized into tumour cells. Under NIR laser irradiation, chromophore PPa generated heat to release chemotherapeutic drugs and generated ROS to exert photodynamic effects. Through cryo-transmission electron microscopy (cryo-TEM), DOX deposits in the vesicles were observed to disappear after laser irradiation, which demonstrated that heat energy allowed the chemotherapeutic drugs to be released (Fig. 8B). After being administered through the tail vein in mice, the vesicles exhibited a slight thermal effect of 45 °C at the tumour site after 10 min of 670 nm laser irradiation, which demonstrated that heat-induced drug release could be achieved *in vivo* (Fig. 8C). More importantly, significant nuclear damage and cytoplasmic degradation were found in the tumour tissue in the treatment group but not in the control groups, which further verified the feasibility of the chromopeptide-based material for chemotherapy combined with phototherapy (Fig. 8D).

In addition, the combination of chemotherapy with phototherapy has overcome the limitations of PDT, *i.e.*, the poor

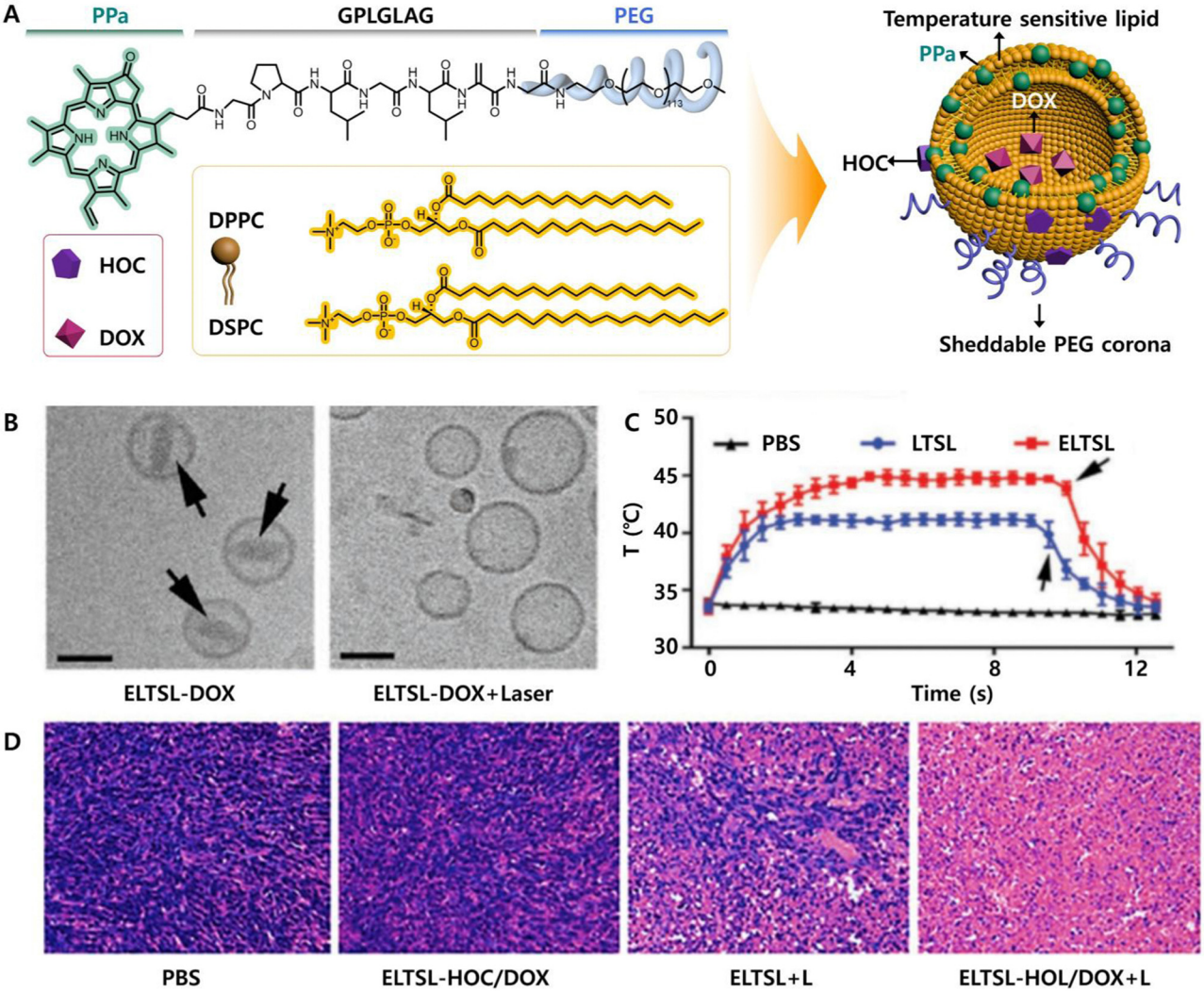

Fig. 8 (A) Chemical structure of the chromopeptide-based chemotherapy combined with phototherapy material with a programmed stimulus-responsive liposome vesicle structure. (B) Cryo-TEM images of the chromopeptide-based material before and after laser irradiation. (C) Photothermal profile of the chromopeptide-based vesicles *in vivo*. (D) H&E staining of the tumour sections in different groups of mice. Reproduced from ref. 121 with permission from [John Wiley and Sons], copyright [2017].

tissue penetration and rapid consumption of oxygen. Kim *et al.* designed a chromopeptide conjugate using the chromophore Ce6, a caspase 3 cleavable peptide (DEVD) and the anticancer drug monomethyl auristatin E (MMAE), which self-assembled into nanoparticles with an average size of 90.8 ± 18.9 nm.[122] Compared with PDT alone, this combined treatment method induced cancer cell apoptosis with a lower irradiation intensity and activated caspase 3 to cleave the anticancer drug MMAE, completing the additional process of killing cancer cells in the absence of a laser.

In the chromopeptide system, some peptides exhibit antitumour effects similar to those of chemotherapy drugs, so these chromopeptide assemblies can also realize the combined effects of chemotherapy and phototherapy without being additionally loaded with chemotherapeutic drugs. Melittin is among the most effective therapeutic peptides and is used as a chemical medicine for treating many diseases, such as cancer.[152,153] However, melittin involves serious haemolysis problems and exhibits nonspecific cytotoxicity. Based on this, Wu *et al.* constructed a chromopeptide supramolecular assembly using melittin, photosensitizer Ce6 and hyaluronic acid (HA).[123] The assembly effectively reduced the side effects of melittin, and Ce6 synergistically promoted the membrane lysis efficiency of melittin with laser irradiation, thus realizing chemotherapy combined with photodynamic antitumour therapy. Although chromopeptide-based nanomaterials can play an important role in the combined treatment of chemotherapy and phototherapy, these materials are useless against highly malignant tumours with metastatic and recurrent tendencies, mainly because these chromopeptide-based nanomaterials cannot effectively accumulate in tumour tissues. Therefore, performing in-depth exploration and development of the active targeting functionality of chromopeptide-based materials is the next goal of this research.

5.3.2 Targeted therapy combined phototherapy. The correct implementation of phototherapy is actually a targeted therapy, which only produces poison in areas in which the photosensitizers accumulate and laser irradiation occurs.[154] However, the method still has limitations, including insufficient targeting, which induces unavoidable side effects in the normal body, such as systemic photosensitivity. With increasing research, in addition to expensive antibodies with large molecular weights, some peptide sequences with small molecular weights and low immunogenicity have been developed to exhibit targeting functions. Therefore, using these peptide sequences with targeting activity to design chromopeptide assemblies will result in great progress towards improving the clinical outcomes of tumour patients.

As the most important cell structure, the nucleus is often the target during material design.[155] Han and co-workers designed a nucleus-targeting amphiphilic chimeric chromopeptide conjugate, including PpIX, a PEG linker and a DMA-modified nuclear localization peptide sequence PKKKRKV, which self-assembled into spherical nanoparticles.[124] The chromopeptide assemblies exhibited a negative charge on the surface and remained stable under physiological conditions. In a tumour microenvironment, because the DMA group responded to acidity, the charge on the assemblies reversed and the surface exhibited a positive charge for nuclear targeting, which accelerated tumour cell interaction. It was observed that many PAPP-DMA nanoparticles entered the nucleus after the cells were incubated for 24 h, while nanoparticles that changed the sequence of targeted peptides remained in the cytoplasm. These chromopeptide assemblies in which the nucleus was the target exhibited a prolonged blood circulation time, achieving maximum drug accumulation in the tumour cell nucleus and effectively reducing the toxic side effects after PDT. Similarly, another group used the nuclear targeting peptide TAT in chromopeptide assemblies to prevent the efflux of light-sensitive chromophore molecules, which occurred due to the presence of *P*-glycoprotein in multidrug-resistant cancers.[125]

To further improve the efficiency of targeted drug delivery, carrier-free self-delivery chromopeptide-based nanorods were designed that target the plasma membrane and cell nucleus.[126] The nanorods were self-assembled by chromopeptide conjugates containing a hydrophobic alkyl chain that can target the plasma membrane, PpIX, a peptide sequence PKKKRKV for nuclear localization, and a hydrophilic PEG chain. Plasma membrane-based targeting of PDT directly induced cell necrosis, enhanced membrane permeability, and increased the cellular uptake of nanorods. Subsequently, with the participation of the nuclear targeting peptide, the *in situ* generation of ROS caused oxidative damage to the DNA chain of cells, achieving an enhanced PDT effect. To improve the biocompatibility of targeted drug delivery systems, researchers also used exosome-modified chromopeptide assemblies (ChiP-Exo) to reduce immunogenicity and systemic toxicity.[129] In addition, the researchers designed a self-delivery chromopeptide-based nanoparticle (M-ChiP) to dually target mitochondria and plasma membranes towards photodynamic tumour therapy.[127]

Some proteins that are overexpressed on the surface of tumour cells are also commonly used as targets for drug delivery. Xu *et al.* chose an amphiphilic iRGD peptide (internalizing RGD, CRGDKGPDC) and chemically modified with hydrophilic Arg, a hydrophobic alkyl chain and a Pro sequence to obtain a new molecule, which self-assembled into spherical nanovesicles.[128] The target receptor of iRGD is the integrin receptor ($\alpha_v\beta_3$, $\alpha_v\beta_5$ and $\alpha_v\beta_1$), which is overexpressed in tumour endothelial cells and tumour cells. After binding to the receptor, iRGD was cleaved by tumour-related proteases, thereby exposing its C-terminus motif (CRGDK/R). Then, the sequence bound to tumour endothelial cells and the tumour cell transmembrane receptor glycoprotein neuropilin-1 receptor (NRP-1) to mediate the penetration of vesicles into the tumour. Therefore, the photosensitizer hypocrellin B (HB) was loaded into iRGD-based vesicle structures to produce chromopeptide assemblies, achieving enhanced photosensitizer accumulation, penetration and PDT. In addition, due to repeated administration, PDT also exhibits side effects that cannot be ignored. Based on iRGD targeted therapy, a chromopeptide conjugate (Ppa-iRGDC-BK01) was designed to solve the potential issue through an iRGD peptide.[62] Chromopeptide conjugates formed a reservoir by self-aggregation at the injection site, while a supermolecular depot was formed after the targeting,

penetration, reactivation of photosensitive molecules and the heat-promoted assembly of body temperature were complete; as a result, the effect of the long-released photosensitizer was achieved and repeated administrations were not necessary.

As a channel for drug delivery systems, tumour blood vessels have also been used as another target by researchers to administer drugs in recent years.[156] As a part of tumour blood vessels, tumour vascular endothelial cells are widely used as targets; the cells exhibit more stable gene expression compared with that of tumour cells and are not prone to drug resistance. In tumour vascular endothelial cells, the vascular endothelial growth factor and its receptors are closely related to tumour angiogenesis and subsequent development.[157,158] Aided by the killing effect of phototherapy, some researchers combined the targeted peptide of vascular endothelial cells with a photosensitive chromophore to obtain chromopeptide conjugates for cancer treatment.[69,159] However, little research has been performed on this vascular-targeted chromopeptide assembly. Although many materials have been designed to target tumour cells, the efficiency of drugs reaching cells after passing through layers of barriers in the body is less than 1%.[160,161] Due to this low drug availability, repeated dosing is necessary, which increases the side effects. Therefore, the material design of chromopeptide assemblies based on tumour vascular targeting can still be further developed.

5.3.3 Immunotherapy combined phototherapy. Phototherapy can cause immune-stimulatory immunogenic cell death (ICD) of tumour cells.[162] In general, the immune synergistic effect against tumours is further enhanced by introducing peptide fragments with immune activity into the chromopeptide system or by regulating the precise assembly of chromopeptides to successfully construct assemblies with virus-like structures.

As a class of immunomodulators, peptides with multiple immunoregulatory functions have the ability to enhance or suppress the body's immune system.[163,164] Yan *et al.* selected two clinically approved water-soluble small molecules, thymopentin TP5 (RKDVY) and ICG, which coassembled into chromopeptide-based supramolecular assemblies (TP5-ICG NFs) for localized combined photothermal immunotherapy against pancreatic cancer (Fig. 9A).[105] A TEM image showed that the assemblies were nanofibre structures (Fig. 9B), which was also consistent with an atomic force microscopy (AFM) image (Fig. 9C). In addition, Fourier transform infrared (FTIR) spectroscopy showed the movement of characteristic wavebands, especially the sulfonic acid group of ICG and the amide group of TP5, which verified that this fibre structure was dominated by hydrogen bonding (Fig. 9D and E). Due to the presence of hydrogen bonds, most of the ICG in the nanostructure prevented unstable alkenes from oxidizing, thereby improving the light stability (Fig. 9F) and photo-to-heat conversion efficiency. Two pancreatic tumour cell lines, Pan02 and BxPC-3, were used to evaluate the *in vitro* photothermal treatment effects of nanofibres. Compared with the laser group alone, the two cell lines showed obvious cell necrosis and apoptosis in the nanofibre treatment group, which demonstrated that the nanofibres are strongly phototoxic (Fig. 9G). The immune analysis results showed that after TP5-ICG NFs treatment, the frequency $CD3^+$ T cells, $CD3^+CD4^+$ T cells and $CD3^+CD8^+$ T cells in the mouse spleen was significantly enhanced compared with those of other controls, indicating that the immunity of the mice was enhanced. The changes in cytokine levels were also measured by flow cytometry. Compared with the control group, the frequency of $CD4^+$ IL-4^+ T cells and $CD8^+$ INF-γ^+ T cells produced by mice in the TP5-ICG NFs group was the highest, which was caused by TP5, demonstrating that TP5 can be effectively delivered through nanofibres to enhance the immune effect. The results of haematoxylin and eosin (H&E) staining showed that organs in the TP5-ICG NFs group did not exhibit metastatic or inflammatory lesions under the effect of immune regulation, while organs in the control group contained metastatic tumour lesions in the liver and spleen. Therefore, the combination of immunotherapy and photothermal therapy can effectively inhibit tumour growth and eliminate metastasis (Fig. 9H). The use of clinically approved drugs in this work has further promoted the practical transformation and application of chromopeptide assemblies, but in addition to its application in the treatment of pancreatic cancer, whether it can be extended to experimental models closer to clinical ones needs further research.

In addition to targeting and immunomodulatory functions, chromopeptide systems can act as antigens. A chromopeptide conjugate (PpIX-PEG(8)-KVPRNQDWL) was prepared by connecting PpIX with an antigen peptide using a PEG(8) linker.[75] The conjugates self-assembled into spherical nanoparticles (PPMA) that exhibited good dispersity and stability and effectively generated ROS. After laser irradiation, nanoparticles in tumour cells produced ROS, which induced necrosis or apoptosis of tumour cells and then further generated an immune response under the stimulation of PDT. In addition, introducing a melanoma-specific antigen peptide (KVPRNQDWL) activated specific cytotoxic T cells, which significantly enhanced the antitumour immune response and effectively inhibited the growth of melanoma in mice. This work shows a good tumour treatment effect, but whether the presence and length of the linker will affect the treatment effect of the chromopeptide has not yet been thoroughly studied. Although progress has been made with chromopeptide-based nanomaterials in phototherapy combined with immunotherapy, in-depth exploration of peptide functions remains necessary. For example, more specific tumour antigen peptides could be found to design more suitable and powerful materials to treat malignant tumours that are difficult to resect or highly metastatic.

In addition, immunotherapy drugs can be integrated with the chromopeptide system into a single platform. Recently, a new molecule was formed by linking an immune checkpoint inhibitor to a chromopeptide conjugate containing the enzyme-responsive peptide sequence DEVD and chromophore PpIX.[98] These molecules self-assembled into nanoparticles with a particle size of approximately 50 nm and achieved a cascade of synergistic immunotherapy and phototherapy antitumour effects. The nanoparticles exhibited good stability in different solutions that simulated physiological environments. In a

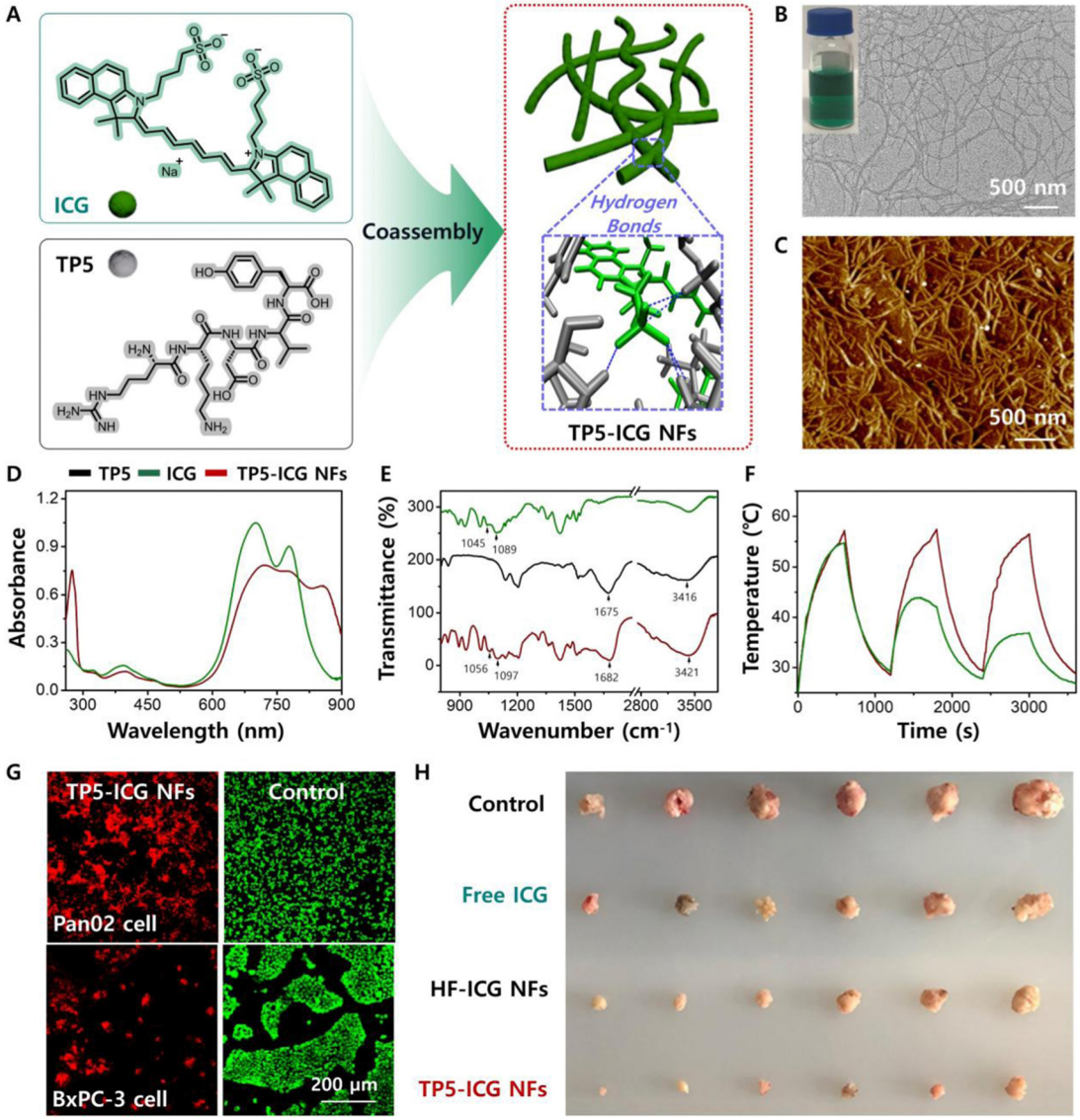

Fig. 9 (A) Schematic illustration of chromopeptide-based supramolecular nanofibres (TP5-ICG NFs) towards localized photothermal immunotherapy. (B) TEM image and (C) AFM image of TP5-ICG NFs. (D) UV-vis absorption spectra and (E) FTIR spectra of free TP5, free ICG and TP5-ICG NFs. (F) Photostability results of free ICG and TP5-ICG NFs. (G) CLSM images of the phototoxicity of TP5-ICG NFs. (H) Photograph of tumours harvested from mice in different groups at 21 days. Reproduced from ref. 105 with permission from [John Wiley and Sons], copyright [2021].

mouse model of lung tumour metastasis established by colon cancer cells, the nanoparticles were passively transported to the tumour site under the EPR effect and generated ROS under laser irradiation to induce cell apoptosis. Subsequently, under the action of caspase-3 in tumour cells, 1MT was released to inhibit the indoleamine-2,3-dioxygenase (IDO) pathway and activate $CD8^+$ T cells. A chromopeptide-based nanoprodrug platform with a core–shell nanostructure was constructed by coassembling the chromophore ICG with a conjugate composed of PEG, a peptide sequence (PVGLIG) and an indoleamine 2,3-dioxygenase (IDO) inhibitor (trade name Epacadostat).[131] In a tumour microenvironment (TME), the PEG layer with a core–shell structure was stripped by matrix metalloproteinase-2 (MMP-2), and its size changed from 140 nm to under 40 nm, which enhanced cellular uptake. Under near-infrared laser irradiation, small-scale nanodrugs convert light energy into heat energy to directly kill tumour cells and generate tumour-related antigens to trigger the immune response. In addition, IDO drugs were released to regulate the T-cell response in the TME, realizing the combination of phototherapy and immune checkpoint blocking therapy. To solve the problems with anti-PD-L1 (the low stability and inability to precisely control the drug loading of the antibody), Luan *et al.* designed a chromopeptide molecule (IR780-M-APP), which was connected by the anti-PD-L1 peptide (APP) and photosensitizer IR780 through peptide segments, and replaced the antibody with APP.[132] These molecules self-assembled into nanoparticles with accurate and controllable APP loading. Under laser irradiation, the nanoparticles exert a photodynamic effect, leading to immunogenic cell death,

which activates the immune response and blocks the PD-1/PD-L1 pathway to promote immunotherapy.

5.4 Biomimetic photocatalysis and photosynthesis

Photocatalysis technology is called ''artificial photosynthesis'', which involves the conversion of light energy into chemical energy in the presence of a catalyst.[7,165–167] The reaction process involves several basic processes, excitation activation, energy transfer, charge separation, electron transfer, and catalytic reaction. Chromopeptides exhibit several advantages, including programmable sequences, tunable self-assembly architecture and ability to easily mimic natural light-harvesting complexes. The light-harvesting, energy transfer, and electron transfer properties generated by chromophore fragments on chromopeptides can be flexibly tuned by peptide-modulated self-assembly (Table 3).

To imitate natural photosynthesis, Park *et al.* selected tetra(hydroxyphenyl) porphyrin (THPP), which exhibits similar optical and electrochemical properties to chlorophyll *a*, as the model light-collecting molecule and adsorbed it onto nanotubes with FF through hydrophobic interactions to simulate natural photosynthetic system I.[168] Compared with a single FF nanotube, the J-aggregate formed by the THPP layer on the surface of the FF nanotube realized stronger exciton coupling between THPP monomers, and its structure is similar to the natural light capture complex containing chlorophyll molecules. Furthermore, Pt nanoparticles (nPt) were deposited on light-harvesting peptide nanotubes through a self-mineralization method to mimic the charge separation function of quinone in natural photosystems. The results also showed that the nanotubes with added Pt successfully promoted the regeneration of NADH and the synthesis of oxidoreductase under visible light. In addition, Yan and Mann *et al.* designed multifunctional biomimetic chromopeptide microspheres by coassembling FF and TPPS to simulate the natural light-harvesting system.[48] To demonstrate the photocatalytic reduction ability of the microspheres, the microsphere solution was irradiated under light for 150 min, and the results showed that 4-nitrophenol (4-NP) could be reduced to 4-aminophenol (4-AP). More importantly, the microsphere structure introduced a higher stability, effectively prevented photodegradation, and could be used as a reasonable photosynthesis model to simulate the energy capture and transformation of primitive abiotic cells.

Inspired by the self-assembly of chromophores that is regulated by natural proteins, Yan *et al.* proposed a strategy to construct a bionic functional system through a peptide-regulated process of porphyrin self-assembly. The researchers constructed a series of chromopeptide systems, manufactured artificial photosystems *via* a molecular self-assembly strategy, and mimicked the architectural principles and functional mechanisms of the photosynthetic system.[48,49,169–171,173,174] For example, they constructed a hierarchical fibre bundle chromopeptide structure with an organization similar to that of pigments in chlorosomes through coassembling peptide KK and TPPS.[49] The surface of the chromopeptide fibre bundle was positively charged, which contributed to the mineralization of TiO_2 nanoparticles. In addition, after the photoreduction of platinum potassium(ii) tetrachloride, the chromopeptide assemblies also promoted the *in situ* mineralization of Pt nanoparticles on the fibre (Fig. 10A). More importantly, when TiO_2/Pt was introduced into the chromopeptide fibre bundle, the whole system generated hydrogen, which was similar to the original reaction centre model, indicating that the chromopeptide assemblies realized the biomimetic structure of the green sulfur bacteria (Fig. 10B).[169] In another example, inspired by pathological processes of cystine stones, the researchers introduced Zn^{2+} metal ions into the chromopeptide system and obtained hierarchically ordered microspheres *via* coordination and hydrogen bonds. These microspheres are formed from the splitting growth of nanorods and can be effectively encapsulated with TPPS and alcohol dehydrogenase (ADH) through electrostatic effects (Fig. 10C). These chromopeptide-based microspheres simultaneously mimicked the structure of grana and the light-dark coupled reactions in chloroplasts, resulting in enhanced sustainability in photocatalytic fuel production (Fig. 10D).[170]

Compared with other biomimetic light-trapping nanostructures, chromopeptide-based materials exhibit good biocompatibility and biodegradability. The chromophore is responsible for light absorption, and the peptide regulates the structure and solubility. Self-assembled nanomaterials of chromophores and peptide conjugates with fixed stoichiometric ratios are also used to enrich biomimetic photosynthetic materials. Collini and co-workers designed a nanoarchitecture by the self-assembly of pyropheophorbide–peptide conjugates, which acted as artificial light harvesters.[175] Among them, the self-assembly of peptide fragments promoted the formation of an exciton network structure that exhibited broad spectral absorption of pigment molecules. The excitation energy of the system could be gathered into a variety of long-life dark states at an ultrafast speed, which showed that the system exhibited great potential for capturing light efficiently. In addition, Gazit *et al.* constructed nanofibre-based multiporous microspheres that exhibited broad-spectrum

Table 3 Summary of chromopeptide assemblies for application in biomimetic photocatalysis and photosynthesis

Chromopeptide-based nanomaterials	Chromophore	Peptide	Morphology	Application	Ref.
FF/porphyrin/Pt	THPP	FF	Nanotubes	Light-harvesting and biomimetic photosynthesis	168
TPPS/FF	TPPS	FF	Hierarchical porous Microsphere	Light-harvesting and photocatalysis	48
TPPS/KK/Pt	TPPS	KK	Fibre	Photocatalysis	49
TPPS/KK/TiO_2/Pt	TPPS	KK	Fibre	Biomimetic photobacteria and H_2 evolution	169
TPPS/Cystine/ADH	TPPS	Cystine	Microsphere	Biomimetic photoenzyme and fuel synthesis	170
TPPS/Fmoc-Leu	TPPS	Fmoc-Leu	Urchin-like microsphere	Light-harvesting	171
MCpP-FF	TPP	FF	Multiporous microsphere	Photosynthesis	172

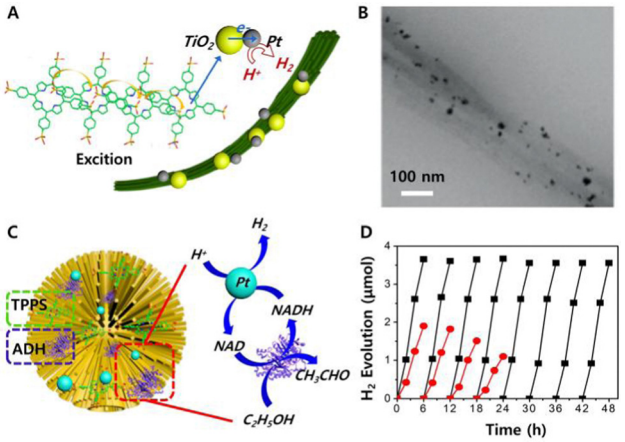

Fig. 10 (A) Schematic diagram of molecular evolution towards mimicking primitive hydrogen-producing photobacteria by self-organization of TPPS and peptides. (B) TEM image of the hybrid fibres showing mineralized nanoparticles. Reproduced from ref. 169 with permission from [John Wiley and Sons], copyright [2015]. (C) Schematic representation of the hierarchical chloroplast mimics fabricated by the Zn^{2+}-directed assembly of cystine with encapsulation of porphyrin and enzyme molecules for photoenzymatic reactions. (D) Time dependence of H2 production on the microspheres in the presence of K_2PtCl_4 and NADH (red line) or K_2PtCl_4, NADH and ethanol (black line). Reproduced from ref. 170 with permission from [John Wiley and Sons], copyright [2016].

photosensitivity and remarkable electron transfer characteristics, and these microspheres were obtained by the self-assembly of a conjugate composed of porphyrin and phenylalanine.[172] Therefore, the microsphere could also be used as an antenna for artificial photosynthesis. Although current biomimetic materials, including chromopeptide-based materials, show high efficiency in light capture, the overall energy efficiency for photosynthesis still remains low. However, their roles in pushing this field forward cannot be ignored. Chromopeptide-based materials provide a reference for further designing simple functional materials to imitate the complex process of natural photocatalysis and photosynthesis. In addition to the chromopeptide assemblies based on porphyrin and its derivatives, the biomimetic photocatalysis and photosynthesis potential of other chromophores such as cyanines still need to be explored.

6. Conclusions

Research studies on chromopeptides and chromopeptide self-assembly have emerged as an attractive and on-developing field (Fig. 11). Chromopeptides are a biologically-derived building block inspired by natural chromoprotein, which integrate the functions of both chromophores and peptides. Because of their elegant molecular structure and flexible design, chromopeptides have been used to construct a variety of self-assembled nanostructures with fascinating functions. The molecular structure of the chromopeptides can be formed by both covalent bonds and noncovalent bonds. Cooperative intermolecular interactions between chromopeptide assemblies lead to particular structures and functions. By precisely and ingeniously designing the molecular structure of the chromopeptides and controlling the key factors in the self-assembly process (thermodynamics and kinetics), the expected nanostructures and material properties can be achieved. The strategy of chromopeptide self-assembly has promoted the development of peptide-based biomedical nanomaterials and biomimetic nanomaterials with integration of optical and biological functions. Their applications in imaging, phototherapy and combination therapy as well as in biomimetic photocatalysis and photosynthesis have been well demonstrated.

Despite the abundant achievements in the study of chromopeptides, challenges still remain in several aspects. One is how to precisely regulate the self-assembly process and chromopeptide structures. Due to the presence of both chromophores and peptide motifs in the chromopeptide system, their assembly behaviors are drastically different due to the variance in the

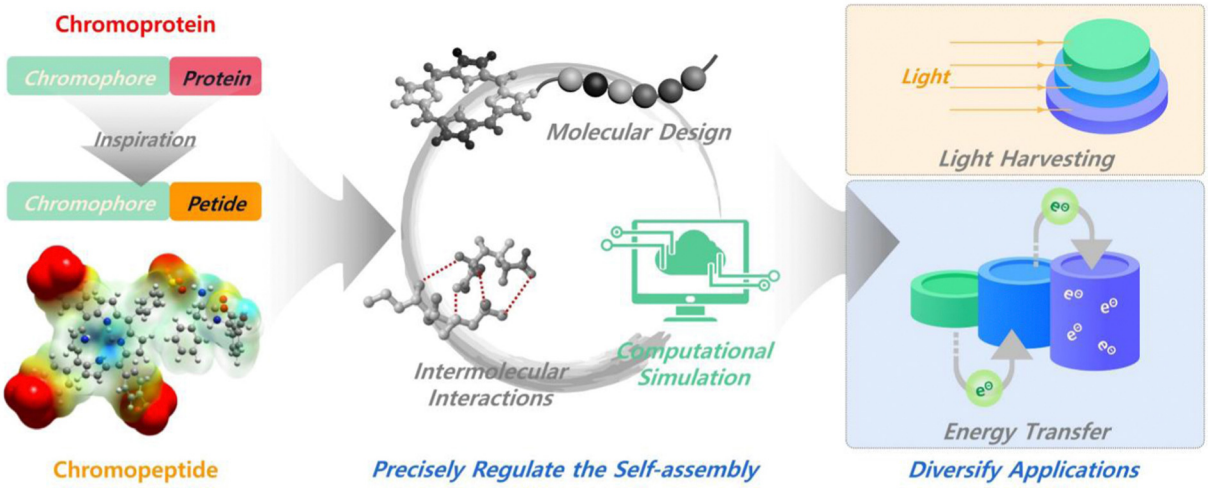

Fig. 11 Functional chromopeptide nanoarchitectonics in retrospect and prospect. More attention should be paid to the computational simulation guided precisely chromopeptide self-assembly regulation, as well as the diversify applications of chromopeptides.

types and strengths of intermolecular interactions. Therefore, regulating the assembly of chromopeptides requires integration of the interaction of the two types of motifs, chromophores and peptides. This undoubtedly greatly increases the technical difficulty of regulating the assembly. In order to achieve the purpose of precise regulation, we believe that, on one hand, it is necessary to pay attention to the design of the chromophore motif, that is, to concentrate on the functionality of the choromophores and their assembly properties, for example, to match their intermolecular interaction strengths with the peptide. Molecular design and synthesis may be required in certain cases. On the other hand, we recommended to make sufficient use of computational simulation to assist molecular design. Both classical molecular dynamics and artificial-intelligence-based prediction have been widely used in peptide sequence design and assembly,[176,177] but rarely in chromopeptides. Establishing a model suitable for the self-assembly of chromopeptides through computational simulation for refining a set of more quantitative structure–activity relationships will greatly benefit. The second challenge is to diversify the application of chromopeptides. Theoretically, chromopeptides can be applied to a wider range of scenarios such as light harvesting, biological charge transport, and energy transfer, in addition to the fields mentioned in this review. However, these applications depend on the properties and functions of chromopeptide assemblies, which in turn are closely related to their supramolecular structures. Limited by the current assembly regulation technique, it is still difficult to realize the applications that require rigorous supramolecular structures of chromopeptides. Thankfully, however, there have been a handful of reports of this kind, albeit abiotic ones.[178–180] Therefore, along with improving precise assembly, it is suggested to fully utilize the biological advantages of natural pigment derivatives and peptides to expand their application scenarios, thereby promoting the diversified development of chromopeptide self-assembly from biomedical and artificial photosynthesis materials to bioengineering technology and industrial products. We believe that chromopeptide assemblies will be designed more flexibly and intelligently as researchers focus more on this burgeoning field.

Conflicts of interest

There are no conflicts to declare.

Acknowledgements

This work was financially supported by the National Science Fund for Distinguished Young Scholars of China (no. 22025207), the National Natural Science Foundation of China (project no. 22232006, 22072154 and 22077122), the Youth Innovation Promotion Association of Chinese Academy of Sciences (no. 2021048) and the National Natural Science Foundation of Hebei Province (no. B2020103025).

Notes and references

1 R. R. Naik and S. Singamaneni, *Chem. Rev.*, 2017, **117**, 12581–12583.
2 M. D. Ward and P. R. Raithby, *Chem. Soc. Rev.*, 2013, **42**, 1619–1636.
3 P. Yin, H. M. Choi, C. R. Calvert and N. A. Pierce, *Nature*, 2008, **451**, 318–322.
4 K. Ariga, X. Jia, J. Song, J. P. Hill, D. T. Leong, Y. Jia and J. Li, *Angew. Chem., Int. Ed.*, 2020, **59**, 15424–15446.
5 K. Ariga, *Int. J. Mol. Sci.*, 2022, **23**, 3577.
6 K. Ariga, *Nanoscale Horiz.*, 2021, **6**, 364–378.
7 Q. Zou, K. Liu, M. Abbas and X. Yan, *Adv. Mater.*, 2016, **28**, 1031–1043.
8 N. G. Gurskaya, A. F. Fradkov, A. Terskikh, M. V. Matz, Y. A. Labas, V. I. Martynov, Y. G. Yanushevich, K. A. Lukyanov and S. A. Lukyanov, *FEBS Lett.*, 2001, **507**, 16–20.
9 V. V. Verkhusha and K. A. Lukyanov, *Nat. Biotechnol.*, 2004, **22**, 289–296.
10 E. Reich, R. M. Franklin, A. J. Shatkin and E. L. Tatum, *Science*, 1961, **134**, 556–557.
11 M. Sono, M. P. Roach, E. D. Coulter and J. H. Dawson, *Chem. Rev.*, 1996, **96**, 2841–2887.
12 D. L. Huffman, M. M. Rosenblatt and K. S. Suslick, *J. Am. Chem. Soc.*, 1998, **120**, 6183–6184.
13 M. M. Rosenblatt, J. Y. Wang and K. S. Suslick, *Proc. Natl. Acad. Sci. U. S. A.*, 2003, **100**, 13140–13145.
14 R. Chang, Q. Zou, R. Xing and X. Yan, *Adv. Therap.*, 2019, **2**, 1900048.
15 H. You, H. E. Yoon, P. H. Jeong, H. Ko, J. H. Yoon and Y. C. Kim, *Bioorg. Med. Chem.*, 2015, **23**, 1453–1462.
16 L. Y. Zhao, Q. L. Zou and X. H. Yan, *Bull. Chem. Soc. Jpn.*, 2019, **92**, 70–79.
17 L. Luan, W. Fang, W. Liu, M. Tian, Y. Ni, X. Chen and X. Yu, *Org. Biomol. Chem.*, 2016, **14**, 2985–2992.
18 G. R. Geier and T. Sasaki, *Tetrahedron Lett.*, 1997, **38**, 3821–3824.
19 K. Liu, R. Xing, Q. Zou, G. Ma, H. Mohwald and X. Yan, *Angew. Chem., Int. Ed.*, 2016, **55**, 3036–3039.
20 H. Abrahamse and M. R. Hamblin, *Biochem. J.*, 2016, **473**, 347–364.
21 R. Bonnett, *Chem. Soc. Rev.*, 1995, **24**, 19–33.
22 A. P. Castano, T. N. Demidova and M. R. Hamblin, *Photodiagn. Photodyn. Ther.*, 2004, **1**, 279–293.
23 M. Abbas, Q. Zou, S. Li and X. Yan, *Adv. Mater.*, 2017, **29**, 1605021.
24 S. Li, R. Xing, R. Chang, Q. Zou and X. Yan, *Curr. Opin. Colloid Interface Sci.*, 2018, **35**, 17–25.
25 R. V. Ulijn and D. N. Woolfson, *Chem. Soc. Rev.*, 2010, **39**, 3349–3350.
26 M. J. Webber, E. A. Appel, E. W. Meijer and R. Langer, *Nat. Mater.*, 2016, **15**, 13–26.
27 S. Zhang, *Nat. Biotechnol.*, 2003, **21**, 1171–1178.
28 S. Fleming and R. V. Ulijn, *Chem. Soc. Rev.*, 2014, **43**, 8150–8177.

29 Y. C. Yu, P. Berndt, M. Tirrell and G. B. Fields, *J. Am. Chem. Soc.*, 1996, **118**, 12515–12520.
30 L. Adler-Abramovich and E. Gazit, *Chem. Soc. Rev.*, 2014, **43**, 6881–6893.
31 Q. Song, Z. Cheng, M. Kariuki, S. C. L. Hall, S. K. Hill, J. Y. Rho and S. Perrier, *Chem. Rev.*, 2021, **121**, 13936–13995.
32 R. P. Cheng, S. H. Gellman and W. F. DeGrado, *Chem. Rev.*, 2001, **101**, 3219–3232.
33 J. Wang, K. Liu, R. Xing and X. Yan, *Chem. Soc. Rev.*, 2016, **45**, 5589–5604.
34 M. Aoudia and M. A. J. Rodgers, *J. Am. Chem. Soc.*, 1997, **119**, 12859–12868.
35 M. Wehner and F. Würthner, *Nat. Rev. Chem.*, 2020, **4**, 38–53.
36 G. D. Scholes, G. R. Fleming, A. Olaya-Castro and R. van Grondelle, *Nat. Chem.*, 2011, **3**, 763–774.
37 R. J. Cogdell, N. W. Isaacs, A. A. Freer, J. Arrelano, T. D. Howard, M. Z. Papiz, A. M. Hawthornthwaite-Lawless and S. Prince, *Prog. Biophys. Mol. Biol.*, 1997, **68**, 1–27.
38 X. Qin, M. Suga, T. Kuang and J. R. Shen, *Science*, 2015, **348**, 989–995.
39 F. Biscaglia and M. Gobbo, *Pept. Sci.*, 2018, **110**, e24038.
40 K. Muller-Dethlefs and P. Hobza, *Chem. Rev.*, 2000, **100**, 143–167.
41 E. R. Johnson, S. Keinan, P. Mori-Sanchez, J. Contreras-Garcia, A. J. Cohen and W. Yang, *J. Am. Chem. Soc.*, 2010, **132**, 6498–6506.
42 A. S. R. Koti and N. Periasamy, *Chem. Mater.*, 2003, **15**, 369–371.
43 L. Zhang and M. Liu, *J. Phys. Chem. B*, 2009, **113**, 14015–14020.
44 M. Sakamoto, A. Ueno and H. Mihara, *Chem. Commun.*, 2000, 1741–1742.
45 M. Sakamoto, A. Ueno and H. Mihara, *Chem. – Eur. J.*, 2001, **7**, 2449–2458.
46 H. C. Fry, L. A. Solomon, B. T. Diroll, Y. Liu, D. J. Gosztola and H. M. Cohn, *J. Am. Chem. Soc.*, 2020, **142**, 233–241.
47 L. K. Solomon, J. B. Kronenberg and H. C. Fry, *J. Am. Chem. Soc.*, 2017, **139**, 8497–8507.
48 Q. Zou, L. Zhang, X. Yan, A. Wang, G. Ma, J. Li, H. Mohwald and S. Mann, *Angew. Chem., Int. Ed.*, 2014, **53**, 2366–2370.
49 K. Liu, R. Xing, C. Chen, G. Shen, L. Yan, Q. Zou, G. Ma, H. Mohwald and X. Yan, *Angew. Chem., Int. Ed.*, 2015, **54**, 500–505.
50 D. A. Mendonca, M. Bakker, C. Cruz-Oliveira, V. Neves, M. A. Jimenez, S. Defaus, M. Cavaco, A. S. Veiga, I. Cadima-Couto, M. Castanho, D. Andreu and T. Todorovski, *Bioconjugate Chem.*, 2021, **32**, 1067–1077.
51 M. Ethirajan, Y. Chen, P. Joshi and R. K. Pandey, *Chem. Soc. Rev.*, 2011, **40**, 340–362.
52 B. C. Kovaric, B. Kokona, A. D. Schwab, M. A. Twomey, J. C. de Paula and R. Fairman, *J. Am. Chem. Soc.*, 2006, **128**, 4166–4167.
53 Q. Zou, M. Abbas, L. Zhao, S. Li, G. Shen and X. Yan, *J. Am. Chem. Soc.*, 2017, **139**, 1921–1927.
54 R. Dosselli, R. Ruiz-Gonzalez, F. Moret, V. Agnolon, C. Compagnin, M. Mognato, V. Sella, M. Agut, S. Nonell, M. Gobbo and E. Reddi, *J. Med. Chem.*, 2014, **57**, 1403–1415.
55 F. Moret, M. Gobbo and E. Reddi, *Photochem. Photobiol. Sci.*, 2015, **14**, 1238–1250.
56 R. Dosselli, C. Tampieri, R. Ruiz-Gonzalez, S. De Munari, X. Ragas, D. Sanchez-Garcia, M. Agut, S. Nonell, E. Reddi and M. Gobbo, *J. Med. Chem.*, 2013, **56**, 1052–1063.
57 J. Zhou, G. B. Qi and H. Wang, *J. Mater. Chem. B*, 2016, **4**, 4855–4861.
58 M. Sibrian-Vazquez, T. J. Jensen, R. P. Hammer and M. G. H. Vicente, *J. Med. Chem.*, 2006, **49**, 1364–1372.
59 Z. Zhou, M. Qutaish, Z. Han, R. M. Schur, Y. Liu, D. L. Wilson and Z. R. Lu, *Nat. Commun.*, 2015, **6**, 7984.
60 P.-C. Lo, J. Chen, K. Stefflova, M. S. Warren, R. Navab, B. Bandarchi, S. Mullins, M. Tsao, J. D. Cheng and G. Zheng, *J. Med. Chem.*, 2009, **52**, 358–368.
61 L. L. Li, Q. Zeng, W. J. Liu, X. F. Hu, Y. Li, J. Pan, D. Wan and H. Wang, *ACS Appl. Mater. Interfaces*, 2016, **8**, 17936–17943.
62 H. J. Cho, S. J. Park, W. H. Jung, Y. Cho, D. J. Ahn, Y. S. Lee and S. Kim, *ACS Nano*, 2020, **14**, 15793–15805.
63 B. Mao, C. Liu, W. Zheng, X. Li, R. Ge, H. Shen, X. Guo, Q. Lian, X. Shen and C. Li, *Biomaterials*, 2018, **161**, 306–320.
64 A. Orosz, G. Mezo, L. Herenyi, J. Habdas, Z. Majer, B. Mysliwa-Kurdziel, K. Toth and G. Csik, *Biophys. Chem.*, 2013, **177–178**, 14–23.
65 G. Ghosh, K. K. Kartha and G. Fernandez, *Chem. Commun.*, 2021, **57**, 1603–1606.
66 E. Nikoloudakis, K. Mitropoulou, G. Landrou, G. Charalambidis, V. Nikolaou, A. Mitraki and A. G. Coutsolelos, *Chem. Commun.*, 2019, **55**, 14103–14106.
67 A. Markowska, A. R. Markowski and I. Jarocka-Karpowicz, *Int. J. Mol. Sci.*, 2021, **22**, 12122.
68 E. N. Carrion, J. Santiago, D. Sabatino and S. M. Gorun, *Inorg. Chem.*, 2017, **56**, 7210–7216.
69 L. Tirand, C. Frochot, R. Vanderesse, N. Thomas, E. Trinquet, S. Pinel, M. L. Viriot, F. Guillemin and M. Barberi-Heyob, *J. Controlled Release*, 2006, **111**, 153–164.
70 S. Zalipsky, *Adv. Drug Delivery Rev.*, 1995, **16**, 157–182.
71 K. Knop, R. Hoogenboom, D. Fischer and U. S. Schubert, *Angew. Chem., Int. Ed.*, 2010, **49**, 6288–6308.
72 W. Rut, K. Groborz, L. Zhang, X. Sun, M. Zmudzinski, B. Pawlik, X. Wang, D. Jochmans, J. Neyts, W. Mlynarski, R. Hilgenfeld and M. Drag, *Nat. Chem. Biol.*, 2021, **17**, 222–228.
73 A. D'Souza A and R. Shegokar, *Expert Opin. Drug Delivery*, 2016, **13**, 1257–1275.
74 A. L. Klibanov, K. Maruyama, V. P. Torchilin and L. Huang, *FEBS Lett.*, 1990, **268**, 235–237.
75 H. Cheng, G. L. Fan, J. H. Fan, R. R. Zheng, L. P. Zhao, P. Yuan, X. Y. Zhao, X. Y. Yu and S. Y. Li, *Macromol. Biosci.*, 2019, **19**, 1800410.

76 K. Han, W. Y. Zhang, Z. Y. Ma, S. B. Wang, L. M. Xu, J. Liu, X. Z. Zhang and H. Y. Han, *ACS Appl. Mater. Interfaces*, 2017, **9**, 16043–16053.
77 P. Kasperkiewicz, Y. Altman, M. D'Angelo, G. S. Salvesen and M. Drag, *J. Am. Chem. Soc.*, 2017, **139**, 10115–10125.
78 E. Ranyuk, N. Cauchon, K. Klarskov, B. Guerin and J. E. van Lier, *J. Med. Chem.*, 2013, **56**, 1520–1534.
79 C. L. Schreiber and B. D. Smith, *Nat. Rev. Chem.*, 2019, **3**, 393–400.
80 C. A. Hunter, *Angew. Chem., Int. Ed.*, 2004, **43**, 5310–5324.
81 A. E. Reed, L. A. Curtiss and F. Weinhold, *Chem. Rev.*, 1988, **88**, 899–926.
82 C. Yuan, W. Ji, R. Xing, J. Li, E. Gazit and X. Yan, *Nat. Rev. Chem.*, 2019, **3**, 567–588.
83 J. Li, J. Wang, Y. Zhao, P. Zhou, J. Carter, Z. Li, T. A. Waigh, J. R. Lu and H. Xu, *Coord. Chem. Rev.*, 2020, **421**, 213418.
84 R. W. Chakroun, F. Wang, R. Lin, Y. Wang, H. Su, D. Pompa and H. Cui, *ACS Nano*, 2019, **13**, 7780–7790.
85 X. Zhao, F. Pan, H. Xu, M. Yaseen, H. Shan, C. A. E. Hauser, S. Zhang and J. R. Lu, *Chem. Soc. Rev.*, 2010, **39**, 3480–3498.
86 H. Chen, K. Shou, S. Chen, C. Qu, Z. Wang, L. Jiang, M. Zhu, B. Ding, K. Qian, A. Ji, H. Lou, L. Tong, A. Hsu, Y. Wang, D. W. Felsher, Z. Hu, J. Tian and Z. Cheng, *Adv. Mater.*, 2021, **33**, 2006902.
87 C. Chen, K. Liu, J. Li and X. Yan, *Adv. Colloid Interface Sci.*, 2015, **225**, 177–193.
88 J. Zhao, R. Huang, W. Qi, Y. Wang, R. Su and Z. He, *Prog. Chem.*, 2014, **26**, 1445–1459.
89 Z. Sun, H. Xie, S. Tang, X. F. Yu, Z. Guo, J. Shao, H. Zhang, H. Huang, H. Wang and P. K. Chu, *Angew. Chem., Int. Ed.*, 2015, **54**, 11526–11530.
90 C. M. Hessel, V. P. Pattani, M. Rasch, M. G. Panthani, B. Koo, J. W. Tunnell and B. A. Korgel, *Nano Lett.*, 2011, **11**, 2560–2566.
91 L. Zhao, Y. Liu, R. Chang, R. Xing and X. Yan, *Adv. Funct. Mater.*, 2019, **29**, 1806877.
92 L. Zhao, Y. Liu, R. Xing and X. Yan, *Angew. Chem., Int. Ed.*, 2020, **59**, 3793–3801.
93 R. Chang, Q. Zou, L. Zhao, Y. Liu, R. Xing and X. Yan, *Adv. Mater.*, 2022, **34**, 2200139.
94 G. F. Luo, W. H. Chen, S. Hong, Q. Cheng, W. X. Qiu and X. Z. Zhang, *Adv. Funct. Mater.*, 2017, **27**, 1702122.
95 L. Zhao, S. Li, Y. Liu, R. Xing and X. Yan, *CCS Chem.*, 2019, **1**, 173–180.
96 L. Zhao, X. Ren and X. Yan, *CCS Chem.*, 2021, **3**, 678–693.
97 D. Zhang, G. B. Qi, Y. X. Zhao, S. L. Qiao, C. Yang and H. Wang, *Adv. Mater.*, 2015, **27**, 6125–6130.
98 W. Song, J. Kuang, C. X. Li, M. Zhang, D. Zheng, X. Zeng, C. Liu and X. Z. Zhang, *ACS Nano*, 2018, **12**, 1978–1989.
99 K. Han, J. Zhang, W. Zhang, S. Wang, L. Xu, C. Zhang, X. Zhang and H. Han, *ACS Nano*, 2017, **11**, 3178–3188.
100 J. Fidel, K. C. Kennedy, W. S. Dernell, S. Hansen, V. Wiss, M. R. Stroud, J. I. Molho, S. E. Knoblaugh, J. Meganck, J. M. Olson, B. Rice and J. Parrish-Novak, *Cancer Res.*, 2015, **75**, 4283–4291.
101 J. Parrish-Novak, K. Byrnes-Blake, N. Lalayeva, S. Burleson, J. Fidel, R. Gilmore, P. Gayheart-Walsten, G. A. Bricker, W. J. Crumb, Jr., K. S. Tarlo, S. Hansen, V. Wiss, E. Malta, W. S. Dernell, J. M. Olson and D. M. Miller, *Int. J. Toxicol.*, 2017, **36**, 104–112.
102 H. W. An, L. L. Li, Y. Wang, Z. Wang, D. Hou, Y. X. Lin, S. L. Qiao, M. D. Wang, C. Yang, Y. Cong, Y. Ma, X. X. Zhao, Q. Cai, W. T. Chen, C. Q. Lu, W. Xu, H. Wang and Y. Zhao, *Nat. Commun.*, 2019, **10**, 4861.
103 R. Xing, Q. Zou, C. Yuan, L. Zhao, R. Chang and X. Yan, *Adv. Mater.*, 2019, **31**, 1900822.
104 B. Sun, R. Chang, S. Cao, C. Yuan, L. Zhao, H. Yang, J. Li, X. Yan and J. C. M. van Hest, *Angew. Chem., Int. Ed.*, 2020, **59**, 20582–20588.
105 S. Li, W. Zhang, R. Xing, C. Yuan, H. Xue and X. Yan, *Adv. Mater.*, 2021, **33**, 2100595.
106 Y. Li, R. C. H. Wong, X. Yan, D. K. P. Ng and P. C. Lo, *ACS Appl. Bio Mater.*, 2020, **3**, 5463–5473.
107 S. Li, L. Zhao, R. Chang, R. Xing and X. Yan, *Chem. – Eur. J.*, 2019, **25**, 13429–13435.
108 S. Y. Li, H. Cheng, W. X. Qiu, L. H. Liu, S. Chen, Y. Hu, B. R. Xie, B. Li and X. Z. Zhang, *ACS Appl. Mater. Interfaces*, 2015, **7**, 28319–28329.
109 K. Stefflova, H. Li, J. Chen and G. Zheng, *Bioconjugate Chem.*, 2007, **18**, 379–388.
110 K. Huang, M. Gao, L. Fan, Y. Lai, H. Fan and Z. Hua, *Biomater. Sci.*, 2018, **6**, 2925–2931.
111 H. Jin, G. Zhao, J. Hu, Q. Ren, K. Yang, C. Wan, A. Huang, P. Li, J. P. Feng, J. Chen and Z. Zou, *ACS Appl. Mater. Interfaces*, 2017, **9**, 25755–25766.
112 H. F. Zhang, K. Maslov, G. Stoica and L. V. Wang, *Nat. Biotechnol.*, 2006, **24**, 848–851.
113 M. H. Xu and L. H. V. Wang, *Rev. Sci. Instrum.*, 2006, **77**, 041101.
114 L. V. Wang and S. Hu, *Science*, 2012, **335**, 1458–1462.
115 Y. Liu, L. Zhang, R. Chang and X. Yan, *Chem. Commun.*, 2022, **58**, 2247–2258.
116 S. Li, W. Zhang, H. Xue, R. Xing and X. Yan, *Chem. Sci.*, 2020, **11**, 8644–8656.
117 J. Li and K. Pu, *Chem. Soc. Rev.*, 2019, **48**, 38–71.
118 C. Liang, L. Xu, G. Song and Z. Liu, *Chem. Soc. Rev.*, 2016, **45**, 6250–6269.
119 Q. Gao, D. Huang, Y. Deng, W. Yu, Q. Jin, J. Ji and G. Fu, *Chem. Eng. J.*, 2021, **417**, 129334.
120 L. Qiu, C. Wang, X. Lei, X. Du, Q. Guo, S. Zhou, P. Cui, T. Hong, P. Jiang, J. Wang, Y. Q. Li and J. Xia, *Biomater. Sci.*, 2021, **9**, 3433–3444.
121 F. Zhou, B. Feng, T. Wang, D. Wang, Q. Meng, J. Zeng, Z. Zhang, S. Wang, H. Yu and Y. Li, *Adv. Funct. Mater.*, 2017, **27**, 1606530.
122 W. Um, J. Park, H. Ko, S. Lim, H. Y. Yoon, M. K. Shim, S. Lee, Y. J. Ko, M. J. Kim, J. H. Park, D. K. Lim, Y. Byun, I. C. Kwon and K. Kim, *Biomaterials*, 2019, **224**, 119494.
123 H. R. Jia, Y. X. Zhu, K. F. Xu and F. G. Wu, *Adv. Healthcare Mater.*, 2018, **7**, 1800380.
124 K. Han, W. Zhang, J. Zhang, Q. Lei, S. Wang, J. Liu, X. Zhang and H. Han, *Adv. Funct. Mater.*, 2016, **26**, 4351–4361.

125 Z. Yu, W. Pan, N. Li and B. Tang, *Chem. Sci.*, 2016, **7**, 4237–4244.
126 H. Cheng, P. Yuan, G. Fan, L. Zhao, R. Zheng, B. Yang, X. Qiu, X. Yu, S. Li and X. Zhang, *Appl. Mater. Today*, 2019, **16**, 120–131.
127 H. Cheng, R. R. Zheng, G. L. Fan, J. H. Fan, L. P. Zhao, X. Y. Jiang, B. Yang, X. Y. Yu, S. Y. Li and X. Z. Zhang, *Biomaterials*, 2019, **188**, 1–11.
128 Y. Jiang, X. Pang, R. Liu, Q. Xiao, P. Wang, A. W. Leung, Y. Luan and C. Xu, *ACS Appl. Mater. Interfaces*, 2018, **10**, 31674–31685.
129 H. Cheng, J. H. Fan, L. P. Zhao, G. L. Fan, R. R. Zheng, X. Z. Qiu, X. Y. Yu, S. Y. Li and X. Z. Zhang, *Biomaterials*, 2019, **211**, 14–24.
130 W. Li, S. Tan, Y. Xing, Q. Liu, S. Li, Q. Chen, M. Yu, F. Wang and Z. Hong, *Mol. Pharmaceutics*, 2018, **15**, 1505–1514.
131 Y. Liu, Y. Lu, X. Zhu, C. Li, M. Yan, J. Pan and G. Ma, *Biomaterials*, 2020, **242**, 119933.
132 N. Wang, Y. Zhou, Y. Xu, X. Ren, S. Zhou, Q. Shang, Y. Jiang and Y. Luan, *Chem. Eng. J.*, 2020, **400**, 125995.
133 J. Liu, S. Chakraborty, P. Hosseinzadeh, Y. Yu, S. Tian, I. Petrik, A. Bhagi and Y. Lu, *Chem. Rev.*, 2014, **114**, 4366–4469.
134 E. Y. Tshuva and S. J. Lippard, *Chem. Rev.*, 2004, **104**, 987–1012.
135 F. A. Armstrong, H. A. Heering and J. Hirst, *Chem. Soc. Rev.*, 1997, **26**, 169–179.
136 Y. Lu, N. Yeung, N. Sieracki and N. M. Marshall, *Nature*, 2009, **460**, 855–862.
137 S. Li, Q. Zou, Y. Li, C. Yuan, R. Xing and X. Yan, *J. Am. Chem. Soc.*, 2018, **140**, 10794–10802.
138 G. J. Kubas, *Acc. Chem. Res.*, 1988, **21**, 120–128.
139 T. J. Meyer, *Pure Appl. Chem.*, 1986, **58**, 1193–1206.
140 M. Li, Y. Ning, J. Chen, X. Duan, N. Song, D. Ding, X. Su and Z. Yu, *Nano Lett.*, 2019, **19**, 7965–7976.
141 X. Lei, L. Qiu, M. Lan, X. Du, S. Zhou, P. Cui, R. Zheng, P. Jiang, J. Wang and J. Xia, *Biomater. Sci.*, 2020, **8**, 6695–6702.
142 H. G. Boman, *J. Intern. Med.*, 2003, **254**, 197–215.
143 Y. Liu, S. Ding, J. Shen and K. Zhu, *Nat. Prod. Rep.*, 2019, **36**, 573–592.
144 S. Lal, S. E. Clare and N. J. Halas, *Acc. Chem. Res.*, 2008, **41**, 1842–1851.
145 Y. Liu, P. Bhattarai, Z. Dai and X. Chen, *Chem. Soc. Rev.*, 2019, **48**, 2053–2108.
146 X. H. Huang, I. H. El-Sayed, W. Qian and M. A. El-Sayed, *J. Am. Chem. Soc.*, 2006, **128**, 2115–2120.
147 F. H. Liu, Y. Cong, G. B. Qi, L. Ji, Z. Y. Qiao and H. Wang, *Nano Lett.*, 2018, **18**, 6577–6584.
148 J. Chen, T. Dai, J. Yu, X. Dai, R. Chen, J. Wu, N. Li, L. Fan, Z. Mao, G. Sheng and L. Li, *Biomater. Sci.*, 2020, **8**, 4447–4457.
149 G. Early Breast Cancer Trialists' Collaborative, *Lancet*, 2005, **365**, 1687–1717.
150 Y. Matsumura and H. Maeda, *Cancer Res.*, 1986, **46**, 6387–6392.
151 L. Kelland, *Nat. Rev. Cancer*, 2007, **7**, 573–584.
152 H. Raghuraman and A. Chattopadhyay, *Biosci. Rep.*, 2007, **27**, 189–223.
153 B. Bechinger, *J. Membr. Biol.*, 1997, **156**, 197–211.
154 Z. Xie, T. Fan, J. An, W. Choi, Y. Duo, Y. Ge, B. Zhang, G. Nie, N. Xie, T. Zheng, Y. Chen, H. Zhang and J. S. Kim, *Chem. Soc. Rev.*, 2020, **49**, 8065–8087.
155 L. Pan, Q. He, J. Liu, Y. Chen, M. Ma, L. Zhang and J. Shi, *J. Am. Chem. Soc.*, 2012, **134**, 5722–5725.
156 D. Hallahan, L. Geng, S. M. Qu, C. Scarfone, T. Giorgio, E. Donnelly, X. Gao and J. Clanton, *Cancer Cell*, 2003, **3**, 63–74.
157 S. Soker, S. Takashima, H. Q. Miao, G. Neufeld and M. Klagsbrun, *Cell*, 1998, **92**, 735–745.
158 D. T. Connolly, D. M. Heuvelman, R. Nelson, J. V. Olander, B. L. Eppley, J. J. Delfino, N. R. Siegel, R. M. Leimgruber and J. Feder, *J. Clin. Invest.*, 1989, **84**, 1470–1478.
159 L. Tirand, N. Thomas, M. Dodeller, D. Dumas, C. Frochot, B. Maunit, F. Guillemin and M. Barberi-Heyob, *Drug Metab. Dispos.*, 2007, **35**, 806–813.
160 L. M. Ellis and D. J. Hicklin, *Nat. Rev. Cancer*, 2008, **8**, 579–591.
161 C. M. Overall and O. Kleifeld, *Nat. Rev. Cancer*, 2006, **6**, 227–239.
162 C. W. Ng, J. Li and K. Pu, *Adv. Funct. Mater.*, 2018, **28**, 1804688.
163 K. Zhao, R. Xing and X. Yan, *Pept. Sci.*, 2020, **113**, e24202.
164 R. Chang and X. Yan, *Small Struct.*, 2020, **1**, 2000068.
165 A. J. Bard and M. A. Fox, *Acc. Chem. Res.*, 1995, **28**, 141–145.
166 M. R. Wasielewski, *Chem. Rev.*, 1992, **92**, 435–461.
167 K. Liu, Y. Kang, G. Ma, H. Möhwald and X. Yan, *Phys. Chem. Chem. Phys.*, 2016, **18**, 16738–16747.
168 J. H. Kim, M. Lee, J. S. Lee and C. B. Park, *Angew. Chem., Int. Ed.*, 2012, **51**, 517–520.
169 K. Liu, R. Xing, Y. Li, Q. Zou, H. Mohwald and X. Yan, *Angew. Chem., Int. Ed.*, 2016, **55**, 12503–12507.
170 K. Liu, C. Yuan, Q. Zou, Z. Xie and X. Yan, *Angew. Chem., Int. Ed.*, 2017, **56**, 7876–7880.
171 K. Liu, M. Abass, Q. Zou and X. Yan, *Green Energy Environ.*, 2017, **2**, 58–63.
172 K. Tao, B. Xue, S. Frere, I. Slutsky, Y. Cao, W. Wang and E. Gazit, *Chem. Mater.*, 2017, **29**, 4454–4460.
173 K. Liu, H. Zhang, R. Xing, Q. Zou and X. Yan, *ACS Nano*, 2017, **11**, 12840–12848.
174 J. Sun, R. Yendluri, K. Liu, Y. Guo, Y. Lvov and X. Yan, *Phys. Chem. Chem. Phys.*, 2017, **19**, 562–567.
175 E. Meneghin, F. Biscaglia, A. Volpato, L. Bolzonello, D. Pedron, E. Frezza, A. Ferrarini, M. Gobbo and E. Collini, *J. Phys. Chem. Lett.*, 2020, **11**, 7972–7980.
176 R. Batra, T. D. Loeffler, H. Chan, S. Srinivasan, H. Cui, L. V. Korendovych, V. Nanda, L. C. Palmer, L. A. Solomon, H. C. Fry and S. K. R. S. Sankaranarayanan, *Nat. Chem.*, 2022, **14**, 1427–1435.
177 P. W. J. M. Frederix, G. G. Scott, Y. M. Abul-Haija, D. Kalafatovic, C. G. Pappas, N. Javid, N. T. Hunt, R. V. Ulijn and T. Tuttle, *Nat. Chem.*, 2015, **7**, 30–37.
178 G. Bullard, F. Tassinari, C. H. Ko, A. K. Mondal, R. Wang, S. Mishra, R. Naaman and M. J. Therien, *J. Am. Chem. Soc.*, 2019, **141**, 14707–14711.
179 M. Di Valentin, M. Albertini, E. Zurlo, M. Gobbo and D. Carbonera, *J. Am. Chem. Soc.*, 2014, **136**, 6582–6585.
180 Q. Song, S. Goia, J. Yang, S. C. L. Hall, M. Staniforth, V. G. Stavros and S. Perrier, *J. Am. Chem. Soc.*, 2021, **143**, 382–389.

